International Journal of Engineering Technologies (IJET)

Volume:10
No:2
June 2025

Printed ISSN: 2149-0104
e-ISSN: 2149-5262

Istanbul Gelisim University Press,
2025

International Journal of Engineering Technologies is an international peer–reviewed journal and published quarterly. The opinions, thoughts, postulations or proposals within the articles are but reflections of the authors and do not, in any way, represent those of the Istanbul Gelisim University.

CORRESPONDENCE and COMMUNICATION:

Istanbul Gelisim University Faculty of Engineering and Architecture
Cihangir Mah. Şehit P. Onb. Murat Şengöz Sk. No: 8
34315 Avcilar / Istanbul / TÜRKİYE
Phone: +90 212 4227000
Fax: +90 212 4227401
e-Mail: ijet@gelisim.edu.tr
Web site: http://ijet.gelisim.edu.tr
https://dergipark.org.tr/en/pub/ijet
Twitter: @IJETJOURNAL

International Journal of Engineering Technologies (IJET) is included in:

International Journal of Engineering Technologies (IJET) is harvested by the following service:

Organization	URL	Starting Date
The OpenAIRE2020 Project	https://www.openaire.eu	2015
GOOGLE SCHOLAR	https://scholar.google.com.tr/	2015
WORLDCAT	https://www.worldcat.org/	2015
IDEALONLINE	http://www.idealonline.com.tr/	2018
ACADEMINDEX	https://www.academindex.com/journals/31	2022
ACARINDEX	https://www.acarindex.com/journals/international-journal-of-engineering-technologies-3765	2022

INTERNATIONAL JOURNAL OF ENGINEERING TECHNOLOGIES (IJET)
International Peer–Reviewed Journal
Volume 10, No 2, June 2025

Owner on Behalf of Istanbul Gelisim University
Rector Prof. Dr. Bahri ŞAHİN

Scientific Advisory Board

From the Editor

Dear Colleagues,

On behalf of the editorial board of International Journal of Engineering Technologies (IJET), I would like to share our happiness to publish the 39th issue of IJET. My special thanks are for members of Editorial Board, Publication Board, Editorial Team, Referees, Authors and other technical staff.

Please find the 39th issue of International Journal of Engineering Technologies at http://ijet.gelisim.edu.tr or https://dergipark.org.tr/en/pub/ijet. We invite you to review the Table of Contents by visiting our web site and review articles and items of interest. IJET will continue to publish high level scientific research papers in the field of Engineering Technologies as an international peer-reviewed scientific and academic journal of Istanbul Gelisim University.

Thanks for your continuing interest in our work,

Prof. Dr. Necmettin MARAŞLI
Istanbul Gelisim University
nmarasli@gelisim.edu.tr

---

http://ijet.gelisim.edu.tr
https://dergipark.org.tr/en/pub/ijet
Printed ISSN: 2149-0104
e-ISSN: 2149-5262


International Journal of
Engineering Technologies
IJET

Table of Contents

Volume 10, No 2, June 2025

International Journal of Engineering Technologies, IJET

e-Mail: ijet@gelisim.edu.tr
Web site: http://ijet.gelisim.edu.tr
https://dergipark.org.tr/en/pub/ijet
Twitter: @IJETJOURNAL

Integration of Natural and Artificial Lighting in Office Spaces to Promote Sustainability

Nahid Babaei*, Semih Göksel Yıldırım**

* Architect (M.Sc.), Institute of Graduate Studies, Istanbul Gelisim University, Cihangir Mahallesi Duygu Sokak No:2 F Block Institute of Graduate Studies, Avcılar, Istanbul, Turkiye, E-mail: nahidbabaei3@gmail.com ORCID: 0009-0003-2048-8357

** Corresponding Author, Assist. Prof., Department of Architecture, Istanbul Gelisim University, Cihangir Mah. Petrol Ofisi Cad. No.5, K Block, 34310, Avcılar, Istanbul, Turkiye. E-mail: sgyildirim@gelisim.edu.tr ORCID: 0000-0002-7832-6575

Received: 23.05.2025 Accepted: 10.07.2025

Abstract- The study examines the methods and technologies employed in integrating natural and artificial lighting in office environments with a focus on sustainability. It explores how artificial lighting can be effectively activated when the illuminance level—an essential aspect of visual comfort—cannot be met by natural light during the day. An example of how natural lighting—defined as a variable light source—can be made energy efficient through automated control systems, when supplemented by artificial lighting, a constant light source, is evaluated in a case study. An office with a renewed spatial organization and an updated automation system was selected for the case study. The analysis focuses on changes in spatial planning, ceiling lighting arrangements, the use of presence and light sensors, and zoning in spatial lighting. The natural lighting is analyzed using computer simulations that compare the previous office layout, PLT 1, with the later layout, PLT 2. Additionally, a partitioned office space is investigated as a preliminary assessment of glare. The evaluation, analysis, and comparisons yield significant findings. Consequently, important insights have been gained regarding the integration of natural and artificial lighting in an office space that has undergone spatial changes and where the automation system has been updated.

Keywords- Office lighting, integrated lighting, daylighting, artificial lighting, lighting performance

Ofis Alanlarında Sürdürülebilirliğe Yönelik Doğal ve Yapay Aydınlatma Entegrasyonu

Öz- Çalışma, sürdürülebilirliğe odaklanarak ofis ortamlarında doğal ve yapay aydınlatmanın bütünleştirilmesinde kullanılan yöntem ve teknolojileri incelemektedir. Gün içinde doğal ışık, görsel konforun temel bir unsuru olan aydınlatma seviyesini karşılayamadığında yapay aydınlatmanın nasıl etkili bir şekilde etkinleştirilebileceğini araştırmaktadır. Değişken ışık kaynağı olarak tanımlanan doğal aydınlatmanın, sabit ışık kaynağı olan yapay aydınlatma ile desteklendiğinde otomatik kontrol sistemleri aracılığıyla nasıl enerji açısından verimli hale getirilebileceğine dair bir örnek, bir vaka çalışmasında değerlendirilmektedir. Yenilenmiş bir mekansal organizasyona ve güncellenmiş bir otomasyon sistemine sahip bir ofis, vaka çalışması için seçilmiştir. Analiz, mekansal planlamadaki değişikliklere, tavan aydınlatma düzenlemelerine, varlık ve ışık sensörlerinin kullanımına ve mekansal aydınlatmada bölgelere ayırmaya odaklanmaktadır. Doğal aydınlatma, önceki ofis düzeni PLT 1' i sonraki düzen PLT 2 ile karşılaştıran bilgisayar simülasyonları kullanılarak analiz edilmektedir. Ek olarak, bölmeli bir ofis alanı parlama için ön değerlendirme olarak incelenmektedir. Değerlendirme, analiz ve karşılaştırmalar önemli bulgular ortaya koymaktadır. Sonuç olarak, mekansal değişime uğrayan ve otomasyon sistemi güncellenen bir ofis mekanında doğal ve yapay aydınlatmanın entegrasyonu konusunda önemli bilgiler elde edilmiştir.

Anahtar Kelimeler- Ofis aydınlatması, bütünleşik aydınlatma, doğal aydınlatma, yapay aydınlatma, aydınlatma performansı

1. Introduction

In contemporary architecture, lighting serves not only to fulfill the basic illumination needs of a space but has also evolved into a design tool that enhances user health, comfort, and performance. Office workers spend a substantial portion of their lives in their work environments. Research indicates that lighting in offices significantly influences workers' well-being and productivity, in addition to its functional role [1, 2]. Maximizing the use of natural light can positively impact human health and performance while also contributing to energy conservation.

Today, advanced technologies that are responsive to user needs and enhance energy efficiency are at the forefront of lighting design. Thanks to light and motion sensors, automated lighting systems can optimize both the intensity

and color of light based on the usage of the space [3, 4]. These systems not only reduce energy consumption but also improve visual comfort by making artificial lighting resemble natural lighting in terms of color and intensity [5, 6]. Through building automation, control over the quantity and timing of lighting in a space can be achieved, allowing customization according to user needs while effectively utilizing artificial lighting [7].

In addition, the division of lighting according to spatial needs (zoning) enhances both environmental quality and user experience. Effective zoning, combined with the use of sensors to integrate natural and artificial lighting in office spaces, can lead to significant energy savings [8, 9]. In office environments, desktop task lighting can help employees maintain focus, while ambient lighting can provide a wide and uniform light distribution in common areas [10, 11]. These technological solutions not only conserve energy but also enhance user satisfaction by allowing for personalized lighting options. Implementing such systems in lighting design represents a contemporary approach that promotes both individual comfort and collective efficiency [5, 6, 12]. Studying the various types of natural and artificial lighting, understanding the distinctions between these two forms, and learning the control methods are essential for creating an effective design that meets the lighting needs of a given space.

The use of natural and artificial lighting in buildings involves various design processes. Natural lighting influences a space in different ways, depending on the time of day and the direction of the light. When natural lighting fails to provide the minimum required illumination for a space, it becomes necessary to supplement it with artificial lighting at varying levels. Generally, natural lighting is categorized into two types: side lighting and top lighting. In contrast, artificial lighting is classified into three types: ambient lighting, task lighting, and accent lighting [10, 13]. Regarding control systems, fixed or movable sunshades are commonly used for natural lighting, while manual or automatic control systems are employed for artificial lighting [13, 14].

The primary challenge is to determine how to achieve the minimum illuminance necessary for visual comfort in spaces that utilize both types of lighting simultaneously. The focus of this study is on integrating these two lighting types in office environments. The research hypothesis posits that the combination of time-varying natural light and controllable artificial lighting, through various methods, can not only ensure the required visual comfort but also enhance energy efficiency in a sustainable manner. Furthermore, these methods and technologies can assist designers and yield valuable insights regarding energy efficiency and human health. Therefore, the aim of this study is to examine the methods used to integrate both types of lighting through a case study. Some of the sub-objectives include identifying relevant design parameters, performance measurement methods, challenges and their solutions, as well as the advantages and limitations of each approach. The lighting performance of the offices analyzed in the case study is evaluated using computer simulations.

2. Materials and Methods

Lighting plays a crucial role not only as a design element but also as a factor that supports health and visual comfort in the workplace. The type of work performed influences the minimum required illuminance [15]. To enhance the productivity and comfort of employees, careful attention should be given to the lighting layout in an office. Visual comfort is generally defined as a subjective response to the quantity and quality of light in a specific space at a particular time. Light levels that fall above or below the required illuminance for a space can lead to visual discomfort [16]. The values necessary for ensuring visual comfort in lighting design are outlined in various international standards, such as EN 12464-1, CIE (International Commission on Illumination), and IES (Illuminating Engineering Society). CIE documents establish standards, relevant regulations, and current research on indoor lighting. It is beneficial to review specific parameters when evaluating integrated lighting [17, 18]. Analyzing the factors that influence visual comfort in office environments and providing general definitions of integrated lighting will help define the scope of the field study to be conducted. It is essential to discuss the topic within the limitations identified from this analysis.

2.1. Factors Affecting Visual Comfort Conditions in Offices

The factors that contribute to visual comfort conditions are defined as illuminance, luminance, and color [19]. The evaluation indices related to this definition are presented in Table 1. According to international standards, the minimum illuminance level for offices should be 300 lux [17]. Comfortable lighting in office spaces is believed to enhance employee performance. When ambient lighting and task lighting are used simultaneously in an office, the average illuminance in non-working areas should not be less than half of the illuminance in the working area. Additionally, the illuminance of the corridor adjacent to the office is expected to maintain a certain proportion of the average illuminance of the office [20]. Otherwise, significant contrasts in luminance levels within the office can lead to visual discomfort or fatigue for workers. The uniformity of the illuminance level within the visual field, specifically the consistent distribution of illumination, significantly impacts visual comfort conditions [21]. The parameters influencing the uniformity factor include the lowest measured illuminance level and the average of the measured illuminance levels [15]. In interior spaces, the distribution of luminance across volume surfaces is a crucial factor for visual comfort. To mitigate the negative effects of luminance distribution and to create an environment conducive to visual perception, specific ratios must be maintained between the luminance of various surfaces and objects within the visual field, ensuring these values remain within established limits [22, 23]. Each surface in the space exhibits different light reflection rates based on its material properties. Some materials produce a brighter appearance by reflecting light at a high rate, while others absorb light significantly, resulting in lower luminosity. This plays a crucial role in the balanced distribution of illuminance within

a space [24]. The amount of visible light transmitted through the glazing system is expressed as a percentage. A low visible light transmittance (VLT) is beneficial for glare control, while a high degree of transmittance is preferred to maintain natural lighting [25, 26]. Several factors influence VLT. Glass coatings can reduce VLT by reflecting and absorbing some of the visible light. Similarly, the use of colored glass diminishes VLT by absorbing or reflecting light. The thickness of the glass is also a significant factor; thicker glass absorbs more light, resulting in a lower VLT compared to thinner glass [27].

Table 1: Visual comfort conditions and evaluation indices in a space [28, 29]. (Table is created by the authors)

Visual Comfort Conditions	Evaluation Index
Illuminance Level	• Minimum required illuminance level (lux)
	• Uniformity ratio (U_0)
Glare	• Surface reflectance ratios used in the space (ρ)
	• Visible light transmittance (VLT) value for glass surface
	• Glare index (UGR)
Color	• Color rendering index (CRI)

In architectural design, offices are categorized into three main types: traditional (cellular) offices, open-plan offices, and group offices as co-working space [30]. The differences in architectural design among these office types also influence artificial lighting design, necessitating distinct solutions. For instance, in open-plan offices, ambient lighting is often designed to provide minimum required illumination for workspaces, which inadvertently illuminates the surrounding circulation areas to the same degree. However, these circulation areas may not require such high levels of illumination. This situation highlights the need for a combination of ambient and task lighting [30]. Furthermore, in traditional (cellular) offices, where spaces are typically smaller, it may be more effective to utilize general lighting throughout the entire area.

Each of the indices presented in Table 1 represents an area that requires individual examination. In a field study, it is considered more appropriate to evaluate one or more of these indices rather than all of them simultaneously. In this context, given the widespread use of computer simulations to assess natural lighting performance, prioritizing the analysis of illuminance levels in any field study is advisable. Additionally, preliminary assessments of glare can be included alongside the sample analysis.

2.2. Definitions of Integrated Lighting

The combination of natural and artificial lighting is referred to as integrated lighting. This definition encompasses the hours during which spaces are actively used throughout the day, excluding the period after sunset when only artificial lighting is employed. Integrated lighting applications are primarily found in public buildings and offices, but they can also be implemented in residential settings. This study focuses specifically on offices as a building type. The primary objective is to ensure that the minimum illuminance levels in offices are achieved through natural lighting during daytime working hours. In instances where natural lighting is inadequate, artificial lighting is employed to supplement and enhance illumination.

Table 2: Overview of integrated lighting (Table is created by the authors).

Light Sources	Features	Controllability	Targets	Challenges
Natural	Dynamic (climate-based)	Difficult (fixed or moving shading device can be used)	Achieving a defined threshold (e.g., DF 2-5% range)	Values above and below the defined threshold are obtained.
Artificial	Static (manual or automatic control system / can be adjustable by occupant)	Easy (by occupancy and daylight sensor and applying zoning in a space)	Supplementing natural light when it fails to meet the desired minimum illuminance level.	The need to implement a building automation system arises from the inefficiency of manual systems.

The artificial lighting used to complement natural light provides a consistent light source. Light sensors, which will be installed in the space, will provide real-time readings of variable parameters related to natural lighting, depending on the time of day and sky conditions [31]. In addition, the brightness level of artificial lighting can be adjusted through

dimming [32]. Zoning can also be implemented within the space, allowing for a controllable process regarding when, how much, and in which areas artificial lighting will complement natural lighting [33]. As part of the control system, both manual and automatic controls are prominent. However, compared to the capabilities offered by automatic control, manual control is less effective. This is because manual control lacks instantaneous illuminance level measurement and the ability for rapid intervention in artificial lighting, as seen in automatic control [14]. There are various types of automatic control systems [3, 4]. In this study, the focus is narrowed to a centralized automation system, presence sensors, and photocell sensors [8, 32, 34]. An overview of integrated lighting is presented in Table 2.

3. Evaluation of Integrated Lighting Applications in a Sample Office

An evaluation has been conducted on a sample office for the application of integrated lighting. The evaluation criteria are based on the information presented in Table 1 and Table 2 in the second section. Table 1 includes the minimum required illuminance conditions and preliminary assessments of glare. Furthermore, the general evaluation of integrated lighting in Table 2 is illustrated through the sample office discussed in this study.

The building analyzed in this case study is located in Istanbul and consists of thirty floors (see Fig. 1). Constructed in 1998, it was originally designed as an office building. However, following a change of ownership in the late 2010s, the building was repurposed for use as a university facility (refer to Fig. 1). This transition necessitated modifications to the spatial layout of the building, transforming it into a mixed-use structure that accommodates both educational and office functions. Consequently, the interior design required reorganization, leading to the conversion of some open-plan offices into traditional (cellular) offices or co-working spaces. Due to this transformation, the old office layout on the 18th floor is referred to as PLT 1 in this study, while the new layout is designated as PLT 2. PLT 1 represents the open-plan office configuration, whereas PLT 2 corresponds to the small co-working space (see Fig. 2). In PLT 2, the group of divided offices is primarily designed as shared spaces for multiple academicians to collaborate. PLT 1 originally included four traditional cellular offices and one large open-plan office. In contrast, PLT 2 has reconfigured the open-plan office into fourteen individual offices, all of which have been converted into small co-working spaces (see Table 3).

Figure 1: Left: K block tower (Google Earth, 2025); Center: General view of the building [35]; Right: 18th floor before renovation (Istanbul Gelisim University Department of Construction Affairs).

In the previous automation system, the ceiling lights across the three floors of the tower building were controlled simultaneously. This approach resulted in excessive energy consumption for the building's lighting. Additionally, managing the lighting for all three floors together created challenges in usability. For the University, which is committed to fostering a sustainable campus, it became essential to revise the control of the ceiling lighting on each floor of the tower to reduce energy costs and enhance user comfort. Consequently, the existing automation system was upgraded. Motion and photocell sensors were integrated into the new lighting control system, establishing an automatic lighting solution. Furthermore, zoning was implemented in the design of the system.

A curtain wall glass facade system is employed on the exterior of the K Block Tower building. The primary source of natural light examined in this study is provided by a side window designed in an arc shape in the plan. Spandrel parts cover both the beam and the parapet surface. Beneath the parapet, there are office cabinets and radiators for the heating system. The gray-blue color of the glass surfaces used in the vision parts of the curtain wall facade harmonizes visually with the color of the sky and optimizes natural light transmittance. To utilize natural light efficiently in buildings, the VLT value is typically selected within a range of 70% to 90%. In this project, a VLT value of 85% is anticipated. This value provides high light transmittance, creating a bright and comfortable environment in the offices. Fig. 2 illustrates the interior view of the curtain glass facade system utilized in the project. Both manual and automatic curtains can be employed for natural lighting control. In automatic systems, light intensity is detected using photocell sensors, which adjust the curtains to open, close, or remain half-open as needed. In contrast, manual systems require user intervention for opening and closing the curtains. Such manual curtains can pose challenges in public spaces, which typically experience high user density. In the tower building, manual curtains were implemented, potentially leading to some issues. However,

during the plan revision, these problems were mitigated by reducing the size of the offices and decreasing the number of users in each space (see Fig. 2). In the interior of the PLT 2 plan type, the office partition walls were constructed using transparent glass, with a matte foil applied to the glass surface. These partition walls extend to the full height of the space. This design choice was made during the automation system renewal process, which involved not only updates to the artificial lighting but also the creation of partitions for ventilation supplied from the ceiling. This approach allows for the separation of indoor air control in the offices. However, this aspect is beyond the scope of this study. The matte foil applied to the interior glass partitions was installed up to the average person's eye level, leaving the upper portion of the glass partition wall transparent to maximize light transmission.

Table 3: PLT 1 and PLT 2 plan types and spatial utilization of the 18th floor of the K block tower building (The plans were obtained from the Istanbul Gelisim University Building Works Department (The table is reproduced from the first author's thesis).

PLT1	PLT2	Spatial Use	
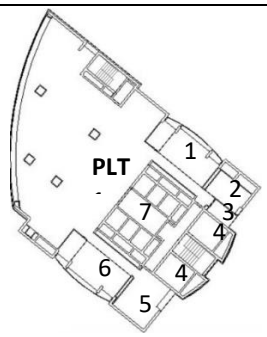	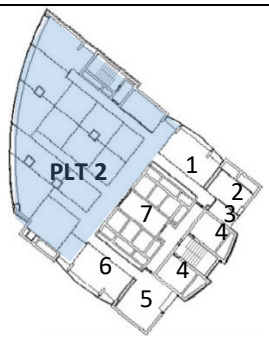	**1**	Office for academician
		2	
		3	Kitchen
		4	Restroom
		5	Office for academician
		6	
		7	Elevator lobby
		PLT1	Open office
		PLT2	Co-working space

Figure 2: The left side features an interior view of the curtain glass facade utilized in the project on the 18th floor. In the center and to the left, roller blinds are employed in the offices. (Photograph by Nahid Babaei)

Table 4: Features of glass partition walls used in the installation of co-working spaces (Photograph by Nahid Babaei)

Glass Partition Wall Features		
Glass type and thickness	4mm single pane	
Type of use	Clear and frosted glass (mixed)	
Light transmittance	85% VLT	
Wall height	260 cm	
Frosted glass height	150 cm	
Transparent glass top band height	110 cm	
Frame material	Aluminum	

Generally, the websites of glass manufacturers indicate that the VLT of frosted glass ranges from 30% to 90%. Low VLT values, such as 30%, offer high privacy while significantly reducing light transmission. In contrast, higher VLT values, such as 90%, allow more natural light to enter, brightening the space but diminishing privacy levels. Medium matte glass, with a VLT of 60%, does not provide complete privacy but permits more natural light to pass through

compared to lower VLT alternatives. However, to minimize light loss, a matte glass with a VLT of 85% was selected instead of medium matte glass. This choice enables sufficient privacy within the office while allowing natural light to efficiently penetrate the space [36]. This predicted value will be utilized in the analyses conducted as a preliminary assessment. The specifications of the glass partition walls used in the installation of the group office / co-working space are presented in Table 4.

In the remainder of the study, firstly, there are findings on artificial lighting that highlight the differences and changes between PLT 1 and PLT 2. These findings focus on ceiling lighting design, control systems, sensor utilization, and zoning. Then, the performance evaluation of natural lighting, which also addresses the differences between PLT 1 and PLT 2, is discussed. Here, the natural lighting is analyzed through computer simulations. Finally, the analysis and evaluation of a group office / co-working space selected from PLT 2 is presented.

3.1. Findings on Artificial Lighting

In the PLT 1 plan layout, a general lighting scheme was implemented in the open office areas without taking into account the interior design and furniture arrangement. The lighting was designed to ensure a uniform distribution throughout the entire space, with no differentiation made between work areas and transitional spaces, such as corridors.

In the PLT 2 plan layout, group office / co-working space were designed, and corridors were created to provide access to these offices. The artificial lighting was zoned, dividing the space into fifteen distinct areas, and the ceiling lighting scheme was restructured. Corridors were designated as a separate zone, with lighting controls implemented to accommodate various usage scenarios. With the renewal of the automation system, presence and illuminance sensors were installed in individual offices, ensuring the integration of natural and artificial lighting. This resulted in the creation of an automatic control system connected to the automation system, which receives real-time data from the spaces and can manage artificial lighting accordingly. Additionally, an independent manual control unit was added for each office, allowing users to adjust the artificial lighting based on their specific needs. This approach aims to enhance user comfort while improving energy efficiency. Thanks to the zonal control units, unnecessary energy consumption is minimized, and the lighting system becomes more adaptable Table 5. illustrates how artificial lighting is segmented in the PLT 1 and PLT 2 plan layouts.

Table 5: Zoning of artificial lighting in the PLT 1 and PLT 2 plan layouts (The plans were obtained from the Istanbul Gelisim University Building Works Department. The table is reproduced from the first author's thesis).

PLT 1	PLT 2
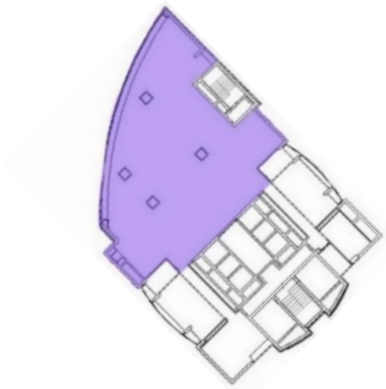	

In the PLT 2 plan layout, the placement of ceiling luminaires has been redesigned and optimized to accommodate the specific lighting requirements and furniture arrangements of the offices. As a result, a more efficient lighting design has been developed, enhancing both visual comfort and energy efficiency. The layout of the ceiling luminaires for artificial lighting in the PLT 1 and PLT 2 layouts is presented in Table 6.

Each office is equipped with a separate wall-mounted switch that allows users to manually control the lighting system. Additionally, the system is designed to respond to the amount of natural light present and features a photo sensor that automatically activates or deactivates the lights based on the ambient light levels. This functionality helps to prevent unnecessary energy consumption, leading to more efficient lighting management. In group offices (co-working spaces), lighting control can be performed both manually and automatically. Users can adjust the lighting using the wall-mounted switch according to their preferences, while the photo sensor monitors the natural light levels and automatically turns the system on or off as needed. The details and operational principles of the lighting control mechanism are presented in Table 7.

In the PLT 2 plan layout, each office is divided into two lighting zones to enhance visual comfort and ensure energy efficiency: luminaires near the windows and those located within the interior. When adequate natural light is available in the space, the lights are automatically turned off, preventing unnecessary use of artificial lighting. It is established that the minimum illuminance at desk level should be 300 lux to maintain visual comfort. If the level of natural light exceeds this threshold, the luminaires closest to the windows are turned

off first, optimizing the use of direct daylight. Conversely, if the level of natural light falls below the threshold, artificial lighting is activated, and the interior luminaires are turned on. This system provides both automatic and manual control, allowing users to adjust the lighting levels according to their personal preferences. Consequently, a balanced and comfortable lighting environment is created, which helps prevent eye fatigue and minimizes reflections and contrast differences.

Table 6: The layouts of ceiling luminaires for artificial lighting in the PLT 1 and PLT 2 plans (The plans were obtained from the Building Works Department of Istanbul Gelisim University. The table is reproduced from the first author's thesis).

PLT 1	PLT 2
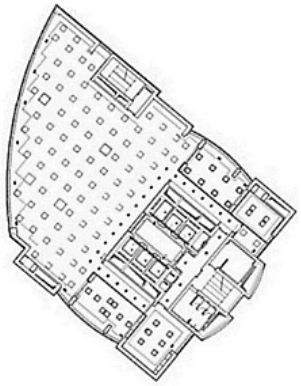	

Table 7: Wall switch for artificial lighting (left) and identification of switch control modes (right). (Photo by Nahid Babaei. The table is reproduced from the first author's thesis.

	Switch Options	Function
	1	On / Off
	2	Photoelectric sensor
	3	Region changes
	4	Automatic dimming
	∧∨	Manual dimming

Table 8: Luminaire models used on the ceiling (Plans were obtained from Istanbul Gelisim University, Department of Construction Affairs. The table is reproduced from the first author's thesis).

PLT 1	PLT 2	
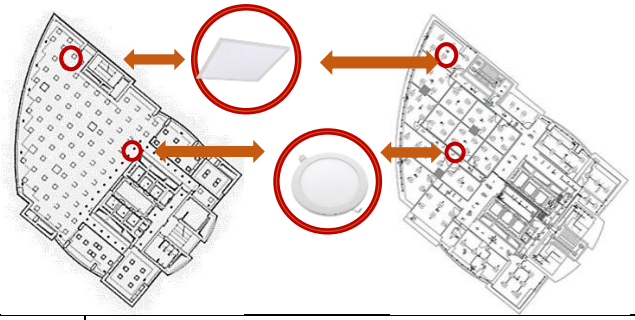		
		**At the entrance, in the corridors and near the window** 18W recessed round LED panel luminaire
		**Group offices (co-working spaces)** 60x60 40W recessed square panel luminaire
		**Open offices** 60x60 24W recessed square panel luminaire

Three models of luminaires were utilized in the PLT 1 and PLT 2 plan layouts. Round lamps were installed at the entrance, in the corridors, and near the windows, while square lamps were employed in the open office and the group offices (co-working spaces). The specifications of the lamps are detailed in Table 8. In the PLT 2 plan layout, round luminaires were implemented throughout all corridors, and 40 W, 60×60 cm square luminaires were preferred for the group offices (co-working spaces). The previous lighting design was revised, and the lighting for each office was designed individually. In the entrance corridor, direct lighting was used on one side, while indirect lighting was applied on the opposite side. Round luminaires were installed in the corridors to ensure adequate illumination throughout the space (see Figure 3).

Figure 3: Ceiling lighting in the corridors of the PLT 2 office layout (Photograph by Nahid Babaei)

3.2. Analyzes of Natural Lighting

In this study, the daylighting performance of PLT 1 and PLT 2 plan types was evaluated through simulations. For the PLT 1 plan layout, the distribution and homogeneity of daylight in the open office spaces were analyzed, along with the impact of natural lighting on the workspaces. In PLT 2, the daylight factor (DF), a static metric, and illuminance, a dynamic (climate-based) metric, were analyzed separately after the open office was converted into group office / co-working space and corridors were established. Since the offices are divided into independent zones, the natural lighting performance of the spaces was comparatively analyzed for both layouts. Simulations for both plan layouts were conducted to assess the efficient use of daylight, determine the need for artificial lighting, and implement optimizations to ensure visual comfort. The data obtained allowed for an evaluation of the effects of different lighting strategies on energy efficiency and user comfort, as well as guidance on how to interpret these findings.

In order to analyze the natural lighting in the offices, the layouts of PLT 1 and PLT 2 on the 18th floor were first modeled using Autodesk Revit. Subsequently, performance evaluations were conducted on the models using the lighting analysis plugin integrated into Autodesk Revit.

3.2.1. DF analysis

The daylighting factor (DF) analyses for the PLT 1 and PLT 2 plan layouts are presented in Table 9. In the PLT 1 plan layout, the average daylight factor (ADF) was calculated to be 3% as a result of the simulation. According to lighting principles, an ADF value in the range of 2% to 5% is considered to provide a sufficient light level. However, artificial lighting may be necessary at certain times. Table 9 displays the illuminance levels for both plan layouts. The total area examined for illuminance levels is 892 square meters. Of this area, 15% falls within the defined thresholds (136 m²), 18% exceeds the threshold (159 m²), and 67% is below the threshold (597 m²). In the PLT 2 plan layout, the ADF was calculated to be 2.8% as a result of the simulation. In this layout, 13% of the area is within the threshold (120 m²), 17% is above the threshold (149 m²), and 70% is below the threshold (623 m²).

There is a 0.2% difference in the ADF value between the PLT 1 and PLT 2 plan layouts. The ADF value is lower in the PLT 2 layout, which is associated with a reduction in the level of natural lighting in the environment. This decrease is attributed to the presence of frosted glass partitions and the limited diffusion of daylight through the glass partition panels (see Table 10).

Table 9. Comparison of DF analysis results across different plan layouts (The table is reproduced from the first author's thesis).

PLT 1	PLT 2
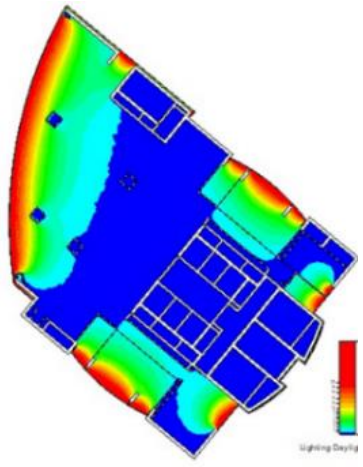	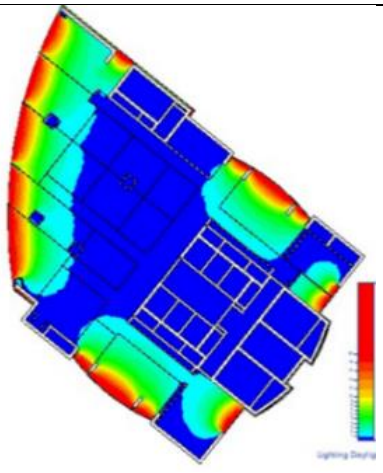

Table 10. Comparison DF analysis data (The table is reproduced from the first author's thesis).

Type of the Plan	ADF	Targeted Threshold		
		Within	Above	Below
PLT 1	%3	%15	%18	%67
PLT 2	%2,8	%13	%17	%70

3.2.2. Illuminance level analysis

The illuminance analysis for PLT 1 and PLT 2 plan types is presented in Tables 11 and 12. To evaluate natural lighting, analyses were conducted on March 21, June 21, and December 21 at 09:00, 12:00, and 15:00. The lighting analyses considered the time periods of 09:00-12:00, 12:00-15:00, and 15:00-18:00 to accurately assess light changes throughout the day. These time periods were selected to observe and analyze variations in natural lighting conditions based on the sun's position. Consequently, the indoor illuminance levels and shaded area distributions at different times can be analyzed more comprehensively.

Table 11: Illuminance level analysis of natural lighting for PLT 1 plan layout (lux) (The table is reproduced from the first author's thesis).

	PLT 1			
	9:00	12:00	15:00	
March 21	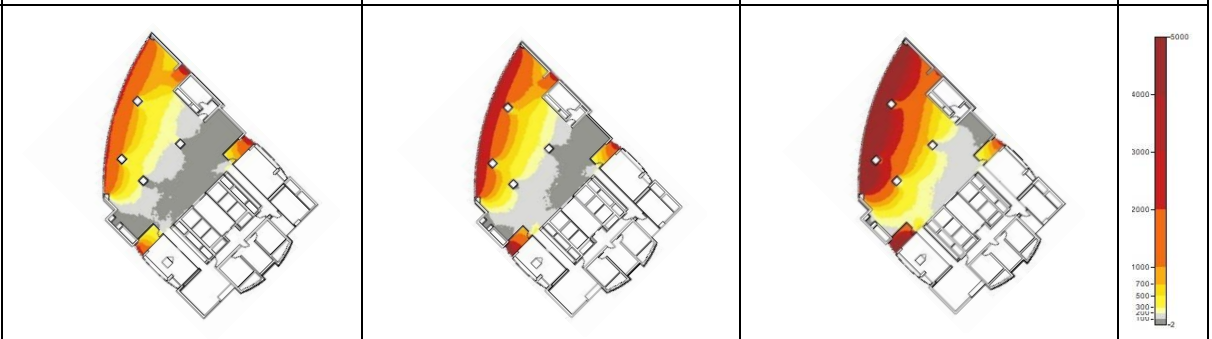			
June 21	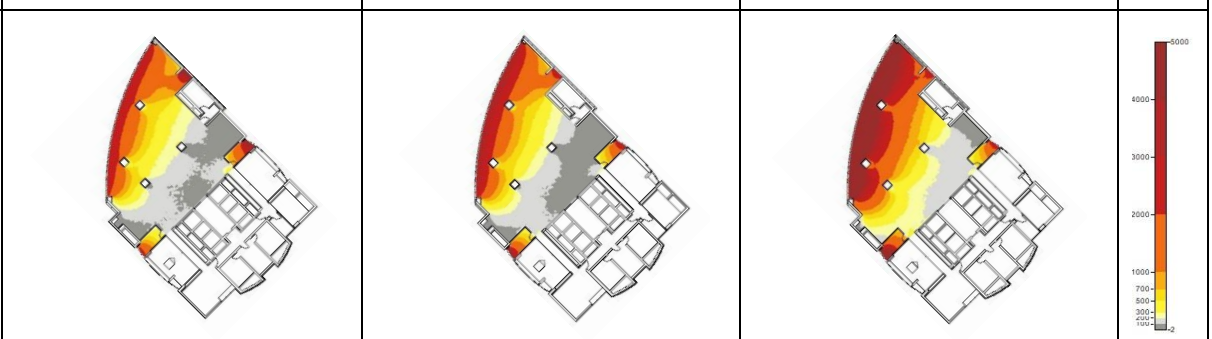			
December 21				

"Perez All-Weather Sky" model is utilized as the sky model in the lighting analysis conducted with Autodesk Revit software. This model is favored for its ability to provide a realistic sky distribution that encompasses all weather conditions. Its capacity to accurately represent sky brightness and light distribution across various atmospheric conditions

allows for reliable results in natural lighting analysis. Specifically, it facilitates a more thorough evaluation by considering factors such as cloud cover, atmospheric conditions, and light variations at different times of the day.

The primary difference between PLT 1 and PLT 2 in this analysis lies in the distribution of light within the space, primarily due to the presence of glass partitions. In the PLT 1 model, light is distributed more uniformly, allowing it to reach areas farther from the window. Conversely, in the PLT 2 model, the partitions partially obstruct the flow of light, leading to a more uneven distribution throughout the space. This results in a greater reliance on artificial lighting in the PLT 2 model. The uneven distribution of natural light within the interior space heightens the dependence on artificial lighting, particularly in areas distant from windows, which consequently leads to increased energy consumption.

Visual comfort is a crucial factor for the productivity and well-being of employees in office environments. In the PLT 1 layout, the larger windows and deeper open office spaces are likely to result in higher levels of glare, particularly in the center near the building core where the elevators are located. Conversely, the PLT 2 layout is expected to have more limited glare levels due to the smaller windows in the group office / co-working space. This situation necessitates conducting detailed glare analyses separately to ensure user comfort. To maintain visual comfort, especially in work areas, it is essential to establish appropriate strategies for controlling daylight.

Table 12: Illuminance level analysis of natural lighting for PLT 2 plan layout (lux) (The table is reproduced from the first author's thesis).

	PLT 2			
	9:00	12:00	15:00	
March 21			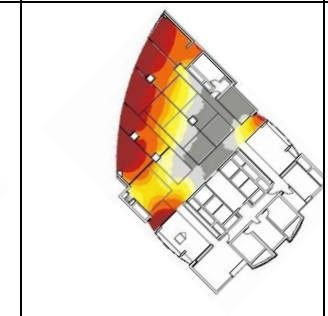	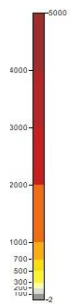
June 21			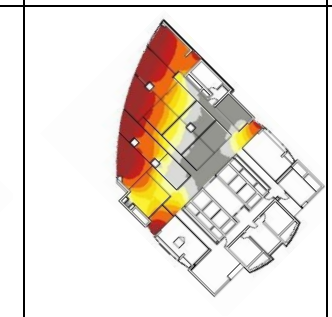	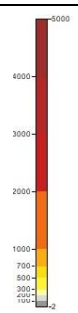
December 21		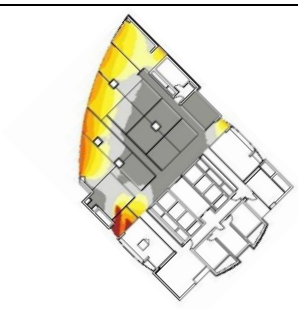		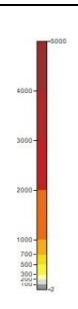

In both plan layouts, high illuminance levels and increased glare effects are typically observed in offices situated near windows. This can adversely impact the visual comfort of employees. Therefore, it is essential to implement lighting control strategies and appropriate shading systems, such as roller blinds. Roller blinds assist in managing daylight, reducing excessive and uncomfortable glare, thereby creating a more pleasant visual environment. Further analyses are necessary to confirm this point conclusively; however, these additional analyses fall outside the scope of this thesis. Future

studies could involve detailed luminance assessments on various days and under different weather conditions to investigate high illuminance levels and potential discomfort caused by glare at the windowsill in a more comprehensive manner.

In both plan layouts, a significant decrease in natural lighting levels is observed in December. This occurs because the sun's rays strike the building at lower angles during the winter months. Consequently, there is an increased reliance on artificial lighting in areas where adequate illumination cannot be achieved through natural light alone. This may necessitate further adjustments to enhance energy efficiency and visual comfort. Among the simulations conducted for various days and times, one was chosen as a representative example, specifically the data from March 21 at 15:00, which fell within the target threshold. The findings from this analysis yield significant insights into lighting performance and regional light distribution. The results and associated data are presented in Table 13.

As a result of the analysis, the areas of the PLT 1 and PLT 2 plan layouts that fall within the target threshold values have been evaluated. In the PLT 1 plan layout, 190 m² of the total area of 415.73 m² was found to be within the threshold values, resulting in a ratio of 45.70%. In the PLT 2 plan layout, the area evaluated within the target threshold value is 174 m², which corresponds to a ratio of 41.85% of the total area.

This data illustrates the distribution of natural and artificial lighting within the space and how the illumination levels in both zones correspond to the established thresholds. The PLT 1 plan layout demonstrates a higher ratio within the target threshold value, resulting in reduced reliance on artificial lighting in this area. In contrast, the PLT 2 plan layout is anticipated to require increased artificial lighting due to its lower target threshold value. This assessment aids in optimizing the lighting design efficiently, ultimately enhancing user comfort.

Table 13: Comparison of luminance level analysis data for the PLT 1 and PLT 2 plan layouts on March 21 at 15:00 (The table is reproduced from the first author's thesis).

Type of the Plan	Area	Targeted Threshold	
		Area	%
PLT1	415,73 m²	190 m²	%45,70
PLT2		174 m²	%41,85

3.3. Analyses and Evaluations of a Group Office / Co-working Space

In the revised plan layout, PLT 2, one independent office has been selected as a case study to analyze the integration of natural and artificial lighting. An office located in the northwest corner of the building, featuring windows on both sides, was chosen for the investigation of lighting levels (see Fig. 4). The simulations utilized specific dates—March 21, June 21, and December 21—at the times of 09:00, 12:00, and 15:00 as parameters for both day and hour. Additionally, the "Perez All Weather Sky" model was employed in all analyses. The objective is to determine the illuminance levels and to make preliminary assessments regarding glare.

The selected office features two windows: one facing northeast and the other facing northwest. According to Table 14, the northeast window experiences higher illuminance levels in the morning, while the northwest window has greater illuminance levels in the afternoon. The analysis indicates that the selected office has lower illuminance levels in December, resulting in a higher demand for artificial lighting compared to other months. Due to the northwest orientation of the office, it receives more natural light between 15:00 and 18:00 among the three different time periods, which can lead to levels that may cause uncomfortable glare.

When the minimum required illuminance cannot be achieved through natural lighting alone, artificial lighting becomes necessary. The office selected as an example is equipped with a photocell sensor that detects natural light levels continuously. When adequate natural lighting is present, the artificial lighting is automatically turned off. However, if the illuminance level drops below a specific threshold, the system automatically activates and turns on the luminaires.

Figure 4: Lighting design of the sample office (The table is reproduced from the first author's thesis).

For artificial lighting, six square lamps are utilized, arranged in pairs across three rows. These lamps can be operated manually or controlled by a motion sensor and photocell (see Table 15).

Table 14: Illumination level and glare analysis of the sample office (The table is reproduced from the first author's thesis).

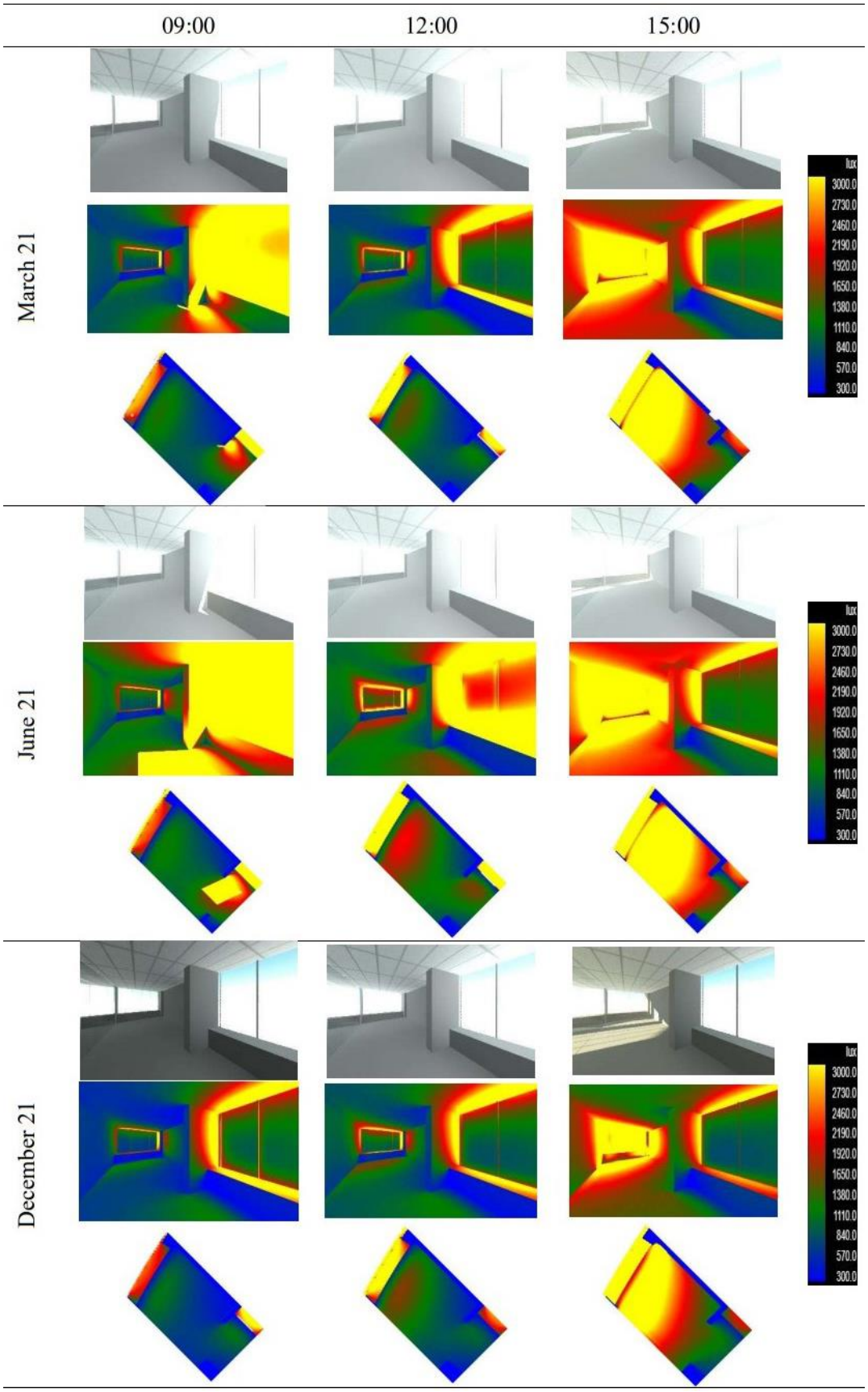

The lighting fixtures in the office are divided into two sections to ensure efficient and balanced illumination. The first section, situated near the windows, receives the most natural light. The second section is located in the central area

of the office, where natural light is minimal. This arrangement enhances visual comfort in the workspace and increases efficiency by reducing unnecessary energy consumption. By optimizing the use of both natural and artificial lighting, this approach not only improves the user experience but also promotes energy efficiency, contributing to sustainability (Fig. 5).

Table 15: Luminaire models used in sample group office / co-working space (The table is reproduced from the first author's thesis).

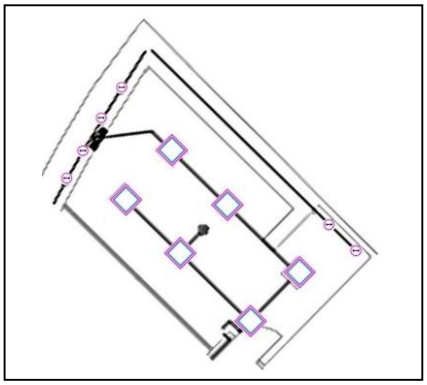

		60x60 40W recessed square panel luminaire
		18W recessed round LED panel luminaire
		Photocell light and motion sensor

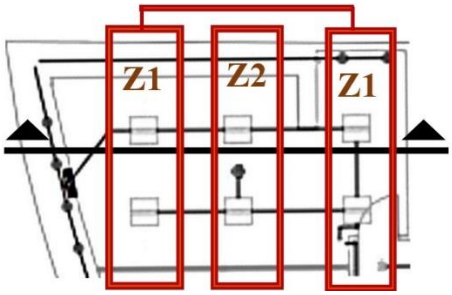

Figure 5: Zoning for the ceiling lighting in the cellular office: the plan of the group office / co-working space is shown on the left, while the section of the group office / co-working space is displayed on the right (The figure is reproduced from the first author's thesis).

On November 18, 2024, two distinct status determinations were made for the group office / co-working space, which was examined through preliminary physical photography. One photograph was taken with the artificial lighting activated, while the other was captured with the lighting deactivated. The images presented in Table 15 offer preliminary data regarding the integration of the artificial lighting system used in the examined group office / co-working space with natural lighting, as well as its interaction with the photocell sensor.

Table 16: A preliminary assessment of natural and artificial lighting in the individual office under review is presented. The left image shows the office with natural lighting only, while the right image displays the office with both natural and artificial lighting (Photograph by Nahid Babaei).

Only with natural lighting (November 18, 2024 – 14:00)	**With natural and artificial lighting (November 18, 2024 – 16:00)**
	

In the left photo of Table 16, it is evident that when natural lighting is adequate, the photocell sensor activates, turning off the lights and conserving energy. In the right photo, it is clear that when natural lighting is insufficient, the photocell sensor activates, turning on the lights to ensure the space is adequately illuminated and providing a uniform light

distribution. These images demonstrate the effectiveness of integrating natural and artificial lighting and highlight the benefits in terms of visual comfort and energy efficiency.

4. Findings from Case Study

DF analyses conducted on the PLT 1 and PLT 2 plan layouts reveal the levels of natural light provided. In the PLT 1 plan layout, the ADF was calculated to be 3%, indicating that natural lighting is generally sufficient, although artificial lighting may be necessary at times. In the PLT 2 plan layout, the ADF was calculated at 2.8%, suggesting an increase in areas that cannot be adequately illuminated by natural light. This indicates a lower level of natural lighting and performance in the PLT 2 plan layout.

In the open-plan offices of PLT 1, excessive light entering from the edges of the windows creates disturbing glare for users in those areas. As less natural light penetrates deeper into the open office, the disparity between the minimum and maximum illumination levels—near the windows—widens, resulting in an increased glare rate. Conversely, in PLT 2, the division of offices reduces the depth of individual workspaces, thereby decreasing the difference between the minimum and maximum illumination levels near the windows. Consequently, the contrast effect and, subsequently, the glare rate diminish. In the centrally located offices, although the natural illumination level is lower, the glare issue is less pronounced, and the light distribution is more balanced. This finding is significant for optimizing lighting strategies and enhancing visual comfort.

In the light level analyses, simulations conducted on different dates (March 21, June 21, and December 21) during specific times of the day reveal how natural light levels in the interior space fluctuate. The analyses assessed whether the light levels in the PLT 1 and PLT 2 plan layouts met the established threshold values. While the PLT 1 plan layout achieved a higher percentage of target threshold value areas (45.70%), the PLT 2 plan layout recorded a rate of 41.85%. This discrepancy suggests that additional artificial lighting is necessary for the PLT 2 plan layout.

Analysis conducted at various times of day reveals how natural light levels fluctuate based on the sun's position. In December, in particular, there was a notable decrease in natural light levels in offices facing northwest due to the lower angles of the sun. This resulted in a greater dependence on artificial lighting, especially in areas distant from windows.

The luminance analyses conducted in the PLT 1 and PLT 2 layouts indicate elevated lux levels and increased glare effects in areas adjacent to the windows. This situation may adversely impact the visual comfort of the workers and requires closer monitoring. It is expected that the glare effect will be more pronounced in the PLT 1 layout due to its larger windows and deeper space, whereas in the PLT 2 layout, glare may be reduced because of the smaller windows and shallower space.

Simulations were conducted to evaluate the effect of sunlight on interior spaces on March 21, June 21, and December 21, at three different times: 09:00, 12:00, and 15:00. The analyses revealed that sunlight penetrates more evenly in the morning and afternoon on March 21 in the PLT1 and PLT2 layout designs. Consequently, this period is considered the most suitable for office use. During midday, however, natural light reaches the center of the plan more limitedly. On June 21, due to the sun's high angle in the sky, the natural lighting level in the space is at its peak. This increase in sunlight can lead to visual comfort issues, such as reflections and glare, as well as heightened thermal loads. Therefore, it is recommended to incorporate shading elements, such as curtains and sunshades, as well as reflective glass. In the PLT 1 plan layout, there is high light intensity throughout the day near the windows. Additionally, the absence of partition panels allows for better distribution of natural light to the interior. In contrast, the PLT 2 plan layout experiences high light intensity only near the exterior facade, resulting in insufficient natural light reaching the interior areas. On December 21, the natural lighting level in the space is at its lowest, with areas that receive adequate light being limited primarily to those close to the north facade. During this time, the demand for artificial lighting increases. To enhance lighting efficiency, it is important to consider the use of light-colored interior surfaces and the strategic placement of furniture.

It was determined that the highest illumination level occurred at 15:00 on March 21st, while the lowest illumination level was recorded at 09:00 on December 21st in both plan layouts. Simulations conducted for March 21st, June 21st, and December 21st revealed that the spaces received more natural light in the afternoon, with the peak illumination level consistently reached at 15:00 among the analyzed hours. A general comparison of illumination levels in the PLT 1 and PLT 2 plan layouts is presented in Table 17.

Table 17: General comparison of lighting in PLT 1 and PLT 2 layouts (The table is reproduced from the first author's thesis).

Features	PLT 1	PLT 2
Light Distribution	Wider and more homogeneous	Limited and concentrated around windows
Area Usage	Large open office, fewer partitions	Small cellular office, more partitions
Efficiency of Natural Light	Medium-low	Medium-low
Brightness of Central Areas	Medium level	Low level

Based on the daylight analyses conducted, it is recommended to incorporate external shading elements to manage the high light intensity in south-facing spaces during the summer months. Simultaneously, an effective natural ventilation system and appropriate thermal insulation should be implemented to prevent overheating that may occur during this period. In the winter months, due to the low levels of natural light, light-colored and reflective surface materials should be favored in interior spaces, and artificial lighting should be strategically planned to enhance illumination levels.

Additionally, considering that daylight is limited in the central areas of the plan, priority should be given to the design of artificial lighting in these regions. The design recommendations should focus on mitigating the negative impacts of seasonal light variations on user comfort, energy efficiency, and overall interior quality. In the PLT 2 variant, the division of office spaces into sections results in offices located far from windows receiving less natural light. Consequently, it was determined that artificial lighting is necessary in all analyzed time zones within these spaces.

In order for natural light to reach the space more effectively, glass with a higher visible light transmittance (VLT) should be preferred over materials with low light transmittance, such as frosted glass. This is particularly important in offices located in the center of the layout, where natural light is limited. Additionally, using artificial lighting with a color temperature and light quality that closely resemble natural light enhances visual comfort for employees and reduces fatigue.

Conclusion

By utilizing dynamic systems that adjust according to the time of day and seasonal changes, offices can provide appropriate lighting for employees at all times. Technologies such as photocells and motion sensors minimize unnecessary energy consumption, ensuring that only the areas in use are illuminated. Achieving energy savings through efficient lighting is a crucial step toward a sustainable future. To maximize the benefits of natural daylight, the placement of windows and the depth of the space should be carefully considered in office designs. In both open office layouts and group office / co-working space configurations, positioning windows on different planes enhances the distribution of natural light, creating a more balanced environment. If the space is equipped with artificial lighting to achieve adequate brightness, dividing ambient lighting into zones is crucial in integrated lighting design. It is essential to provide solutions tailored to the specific lighting needs of each zone. For instance, ambient lighting can be designed differently for areas near windows compared to those farther away. Additionally, focused solutions, such as task lighting in high-traffic work areas, can be combined with ambient lighting to enhance functionality.

The minimum brightness requirements vary depending on the intended use of the spaces. In interior design, various strategies are employed to achieve the desired brightness levels across different surfaces. By considering employee preferences, the intensity, color temperature, and arrangement of lighting can be optimized. Furthermore, a healthier and more comfortable environment can be established by utilizing human-centered lighting systems that support the biological clock and replicate the effects of natural light. Computer-aided simulations can be employed during the planning phase of lighting designs. These simulations help minimize design errors by visualizing the impact of light sources and materials on the space in advance.

This research demonstrates that natural and artificial light can be effectively integrated through various technologies and methods to enhance visual comfort in office environments. However, more comprehensive studies are necessary to thoroughly analyze visual comfort. Specifically, the levels of brightness and glare in each office, along with their effects on visual comfort, should be examined in greater detail. The choice of materials significantly impacts the lighting efficiency of interior spaces. The ability of surfaces to absorb or reflect light can directly influence the distribution of natural light within the area and overall visual comfort. Additionally, the effects of materials used—such as those for floors, walls, and ceilings—on light reflection, as well as the role of this reflection in determining the general brightness level of the environment, should also be taken into account. Therefore, it is beneficial to examine the light reflection properties of the materials used, the effects of lighting conditions on the space, and overall visual comfort. Additionally, a more detailed analysis of how light is distributed in various areas and the impact of this distribution on users can be conducted. These supplementary analyses can enhance office designs and lighting strategies, providing crucial data to improve the user experience. It has been established that more in-depth analyses are necessary regarding glare, another aspect of visual comfort. Furthermore, comparing the energy loads of the sample office building after the automation system has been updated with its previous state will serve as a significant assessment of energy efficiency. Consequently, these additional analyses recommended for future studies can positively contribute to achieving optimal visual comfort and the development of sustainable lighting solutions.

Information Notes

This article is based on the MSc. thesis of the first author at Istanbul Gelisim University, Institute of Graduate Studies, Architecture Master of Science Program, under the supervision of the second author.

The lighting analysis for the case study discussed in the article was conducted by using Autodesk Revit®. The software mentioned is legally used by the authors for educational purposes.

There is no need for ethics committee approval in this article.

Declaration of Conflicting Interest

The authors declared no potential conflicts of interest with respect to the research, authorship, and/or publication of this article.

References

[1] Gentile N., Lee, E. S., Osterhaus, W., Altomonte, S., Amorim, C. N. D., Ciampi, G., Garcia-Hansen, V., Maskarenj, M., Scorpio, M., & Sibilio, S., Evaluation of integrated daylighting and electric lighting design projects: Lessons learned from international case studies. *Energy and Buildings*, 268 (2022), 112191, pp. 1-22, 2022.

[2] Reinhart, C. F. & LoVerso, V. R., A rules of thumb-based design sequence for diffuse daylight. *Lighting*

Research & Technology, vol. 42, issue 1, pp. 7–31, 2010.

[3] Chun, S. Y., Lee, C. S. & Jang J. S., Real-time smart lighting control using human motion tracking from depth camera. *Journal of Real-Time Image Processing*, vol. 10, pp. 805–820, 2015.

[4] Chung, T. M., & Burnett, J., On the prediction of lighting energy savings achieved by occupancy sensors. *Energy Engineering*, vol 98, issue 4, pp. 6–23, 2001.

[5] Designing Buildings, Artificial lighting. Retrieved November 15, 2024, from https://www. designingbuildings.co.uk/wiki/Artificial_lighting, 2021.

[6] Tazemahalle, K. A., Aydınlatma tasarımı ilkelerini tanımak. *Tarrah Publication*, Tahran, 2018.

[7] Tao, L., Integration for daylight and electric lighting plays an important role for NZEB. *IEA (International Energy Agency) SHC (Solar Heating & Cooling Programme) Task 61 Subtask D*. Retrieved November 15, 2024, https://task61.ieashc.org/Data/ Sites/1/publications/CN-CABR.pdf, 2022.

[8] Pandharipande, A., & Li, Sh., Light-harvesting wireless sensors for indoor lighting control. *IEEE Sensors Journal*, vol. 13, no. 12, pp. 4599–4606, 2013.

[9] Kelly, K., & O'Connell, K., Interior lighting design; a student's guide. Retrieved from July 30, 2024. https://abs.cu.edu.tr/Dokumanlar/2016/EEE463/495694447_lightingdesignstudentsguide.pdf, (n.d.).

[10] Çetin, E., Aydınlatma tekniği. *Ders notları*. Bozok University. Retrieved November 15, 2024, from https://muhaz.org/pars_docs/refs/113/112385/112385.pdf, 2018.

[11] Philips, Basics of light and lighting. *Published by Koninklijke Philips Electronics*, New York, 2008.

[12] Galasiu, A. D, Newsham, G. R., Suvagau, C., & Sander, D. M., Energy saving lighting control systems for open-plan offices: a field study. *LEUKOS The Journal of Illuminating Engineering Society*, vol. 4, no 1, pp. 7-29, 2007.

[13] Egan, M. D. & Olgyay, V., Architectural lighting. *Published by McGraw-Hill*, London, 2002.

[14] IEA, Light's labour's lost; Policies for energy-efficient lighting. *Published by IEA (International Energy Agency)*, Paris, France, 2006.

[15] Özkaya, M. & Tüfekçi, T., Aydınlatma tekniği. *Birsen Publication*, İstanbul, Turkiye, 2011.

[16] Gale, J. E., Cox, H. I., Qian, J., Block, G. D., Colwell, C. S. & Matveyenko, A. V., Disruption of circadian rhythms accelerates development of diabetes through pancreatic beta-cell loss and dysfunction. *Journal of Biological Rhythms*, vol. 26, issue 6, pp. 467-478, 2011.

[17] CEN, EN 12464-1, Light and lighting - Lighting of work places – Part 1: Indoor work places. *Publication of the European Committee for Standardization (CEN)*, Brussel, 2022.

[18] Yücel, Ş. B., Açık planlı ofislerde aydınlatma tasarımının irdelenmesi. *MSc. Thesis*, Yıldız Technical University, İstanbul, Turkiye, 2019.

[19] Küçükdoğu, M. Ş., İklimsel konfor ve aydınlık seviyesine bağlı görsel konfor gereksinimleri açısından, pencerelerin tasarlanmasında kullanılabilecek bir yöntem. *PhD Thesis*, Istanbul Technical University, Turkiye, 1980.

[20] CIBSE, Code for lighting (LG7: Office lighting). *Published by CIBSE (Chartered Institution of Building Services Engineers)*, London, 2012.

[21] Dilaura, D. L., Houser, K. W., R.G. Mistrick, R. G., & Steffy, G. R., The lighting handbook; reference and application. *Published by IESNA (Illuminating Engineering Society of North America)*, Tenth Edition, New York, 2011.

[22] Lim, G. H., Hirning, M. B., Keumalaa, N., & Ghafar, N. A., Daylight performance and users' visual appraisal for green building offices in Malaysia. *Energy and Buildings*, 141 (2017), pp. 175–185, 2017.

[23] Yağmur, Ş. A. & Sözen, M. Ş., Visual comfort parameters for classrooms and the effect of interior surfaces. *Megaron*, vol. 11, issue 1, pp. 49–62, 2016.

[24] Eaton, Lighting design guide. *Published by Eaton's Cooper Lighting and Safety Business*, South Yorkshire, UK, 2013.

[25] Baker, N. V., Fanchiotti, A., & Steemers, K., Daylighting in architecture; a European reference book. *Published by Routledge*, London, 1993.

[26] Modaresnezhad, M., A comparative study of workstation partitions in an existing side-lit open plan office with daylight results using annual climate-based simulations. *MSc. Thesis*, University of North Carolina at Greensboro, 2016.

[27] Visible light transmittance (VLT). *Cardinal glass industries*. Retrieved July 30, 2024, from https://www.cardinalcorp.com/glossary/visible-light-transmittance-vlt/ , (n.d.).

[28] Makaremi, N. Schiavoni, S., Pisello, A. L., & Cotana, F., Effects of surface reflectance and lighting design strategies on energy consumption and visual comfort. *Indoor and Built Environment*, vol. 28, no. 4, pp. 552-563, 2018.

[29] Singh, R., & Rawal, R., Effects of surface reflectance on lighting efficiency in interiors. *Proceedings of Building Simulation 2011: 12th Conference of International Building Performance Simulation Association*, Sydney, 14-16 November, 2011.

[30] Gezersu, A. Yeşil ofislerde aydınlatma sistemleri. *MSc. Thesis*, Marmara University, İstanbul, Turkiye, 2019.

[31] Cheng, Y., Fang, C., Jingfeng Yuan, J., & Zhu, L., Design and application of a smart lighting system based on distributed wireless sensor networks. *Applied Sciences*, 10 (2020), 8545, pp. 2-21, 2020.

[32] Roisin, B., Bodart, M., Deneyer, A. & D'Herdt, P., Lighting energy savings in offices using different control systems and their real consumption. *Energy and Buildings*, vol. 40, issue 3, pp. 514–523, 2008.

[33] Christel, B., Mariëlle, A., Helianthe, Kort, E., & Alexander, R., Preferred luminance distributions in open-plan offices in relation to time of day and subjective alertness. *LEUKOS The Journal of Illuminating Engineering Society*, vol. 17, no 1, pp. 3-20, 2019.

[34] Rubinstein, F. M., & Karayel, M., The measured energy savings from two lighting control strategies. *IEEE Transactions on Industry applications, vol* IA-20, issue 5, pp. 1189-1197, 1984.

[35] İstanbul Gelisim University K Block. Retrieved July 30, 2024, from https://gelisim.edu.tr/icerik/istanbul-gelisimuniversitesi-k-blok, (n.d.).

[36] Frosted Window Films. *Contra Vision*. Retrieved January 15, 2025, from https://www.contravision.com/privacy-window-film/frosted/, (n.d).

Improving Cellular Traffic Prediction with Temporal Embeddings: A Time2Vec-LSTM Approach

Hamidullah Riaz[*, ‡], Sıtkı Öztürk[**], Peri Güneş[***]

[*, **] Department of Electronics and Communication, Faculty of Engineering, Kocaeli University, Izmit, Kocaeli, 41001, Türkiye.

[***] Department of Electrical and Electronics, Faculty of Engineering and Architecture, Istanbul Gelisim University, Avcılar, Istanbul, 34310, Türkiye.

(hamidullah.riaz@kocaeli.edu.tr, sozturk@kocaeli.edu.tr, pgunes@gelisim.edu.tr)

(ORCID: 0000-0001-5275-9922 ; 0000-0003-3804-5581 ; 0009-0002-9080-3239)

[‡] Corresponding Author; Kocaeli University, Izmit, Kocaeli, 41001, Türkiye, hamidullah.riaz@kocaeli.edu.tr

Received: 08.05.2025 Accepted: 08.08.2025

Abstract- The network traffic prediction has to be reliable for better resource allocation and congestion management in present-day telecommunications. In this paper, a novel hybrid Time2Vec-enhanced LSTM method is presented for somewhat more accurate traffic volume forecasting. The model exploits both historical traffic behavior and temporal features enriched by Time2Vec, such as hour and day, to represent the linear or periodic dependencies embedded in cellular traffic. Unlike traditional static time encodings or raw time features, the learnable Time2Vec embeddings enable the model to better capture daily and hourly fluctuations in network traffic. The study carried out experiments with a real-world dataset that had been collected from an LTE base station located in Kandahar Province of Afghanistan, with hourly uplink, downlink, and total traffic volumes recorded for 30 days. Performance was measured in terms of the Root Mean Square Error (RMSE) and coefficient of determination (R^2). The results show that the proposed Time2Vec-enhanced LSTM consistently outperforms Deep Learning (DL), statistical, and Machine Learning (ML) models across all traffic types. The learnable temporal embeddings are useful as they allow greater accuracy and better capture of trends. Ablation studies have supported that forecasting is far better with adaptive Time2Vec encoding than with models without or with a fixed-time feature, suggesting that learnable temporal features are essential for precise and robust cellular traffic prediction.

Keywords- Cellular traffic prediction, Deep learning (DL), LSTM, Machine learning (ML), Real-word dataset, Time2Vec.

1. Introduction

The rapid growth of internet and mobile technologies, along with the increasing use of smartphones and other connected devices, has brought about a new era of big data. This has led to a sharp rise in global mobile data usage, which is expected to reach 403 exabytes (EB) per month by 2029 [1]. The growing number of users, applications, and services is putting pressure on communication networks. By the end of 2023, mobile data traffic, excluding fixed wireless access, was estimated at 130 EB per month, with forecasts suggesting this could climb to 563 EB per month by 2029 when fixed wireless is included. At the same time, 5G networks were predicted to carry 25% of this traffic by the end of 2023, increasing significantly to 76% by 2029 [2], [3]. These trends highlight the urgent need for accurate forecasting methods to support better planning, traffic control, and efficient use of resources, while also improving the quality of service for users.

As mobile data usage continues to increase, managing network capacity effectively becomes more difficult. One key solution is accurate prediction of cellular network traffic, which supports better network operations. Being able to anticipate

traffic patterns can help avoid congestion, improve security, and guide the efficient distribution of bandwidth. It also plays a central role in long-term planning by allowing network providers to prepare for future demands. With reliable forecasting, service providers can make more informed decisions and optimize their infrastructure to deliver a smoother and more secure user experience [4].

Cellular traffic prediction is generally divided into temporal and spatiotemporal approaches. Temporal prediction focuses on forecasting traffic at a single location using only its historical data, typically modeled as a univariate time series. In contrast, spatiotemporal prediction captures both temporal patterns and spatial dependencies across network elements, for example base stations, which are influenced by factors such as user mobility and handovers. Based on the number of predicted variables, traffic forecasting can be classified as univariate or multivariate. Univariate methods predict a single variable, such as traffic volume, while multivariate methods forecast multiple related indicators, such as traffic volume and the number of connected users, which often influence one another. Forecasting is also categorized by duration, with short-term prediction typically covering 5 to 60 minutes and medium-to-long-term prediction extending beyond 60 minutes, depending on the data's time granularity. Additionally, predictions may be single-step, focusing on the next time point, or multi-step, predicting traffic over several future intervals [5], [6].

However, despite advances in Machine Learning (ML) and Deep Learning (DL), many existing models still rely on static or hand-engineered time features, which limits their ability to adapt to the complex, variant nature of cellular traffic. To address this limitation, we explore the use of learnable temporal embeddings as a more flexible and data-driven alternative to traditional time encodings.

The aim of the study is to incorporate the Time2Vec mechanism within an LSTM-based architecture for cellular traffic forecasting. Time2Vec is a learnable temporal embedding that represents time as a vector with linear and periodic components. Unlike static encodings, Time2Vec allows the model to automatically discover and adapt to recurring and drifting temporal patterns within the data. To the best of our knowledge, this is the first study to apply Time2Vec in the context of cellular traffic prediction.

Our Time2Vec-enhanced LSTM architecture, by embedding temporal information in a manner that can be learned simultaneously with traffic patterns, will thus provide better temporal awareness and more accurate predictions. We in turn validate this model on actual LTE traffic data collected from a live cellular network, demonstrating that it consistently outperforms a diverse range of methods including DL approaches such as LSTM and GRU, traditional time series model such as Auto-Regressive Integrated Moving Average (ARIMA), and classical ML techniques such as Support Vector Regression (SVR) and Random Forest (RF). This highlights the potential of combining sequence modeling with a powerful temporal embedding to improve the robustness and accuracy of cellular traffic forecasting.

The key contributions of this work are as listed below:

- We propose a hybrid Time2Vec-enhanced LSTM model where learnable temporal embeddings are incorporated for sequential modeling to gain higher accuracy in cellular traffic forecasting.
- We introduce Time2Vec into the telecom traffic prediction field, demonstrating that it offers superior performance compared to traditional static time encodings or raw time features, particularly for modeling daily and hourly fluctuations in network traffic.
- We validate the model on actual LTE traffic data collected from a base station in Afghanistan, featuring uplink, downlink, and total traffic volume, all recorded hourly over 30 days.
- We conduct comprehensive empirical comparisons with DL models (LSTM and GRU), traditional statistical (ARIMA), and ML models (SVR and RF), demonstrating that our proposed model consistently achieves lower Root Mean Square Error (RMSE) and higher coefficient of determination (R2) across all traffic types.

The remainder of the paper is organized as follows: Section 2, Section 3 describes the Materials and Methods, including the dataset, LSTM architecture, and Time2Vec embedding. Section 3.3 presents the Proposed Model. Section 4 discusses the Results and Analysis, and finally, Section concludes the paper.

2. Related Work

The task of forecasting traffic in cellular networks has traditionally been addressed using statistical time-series models such as ARIMA [7] and Seasonal ARIMA (SARIMA) [8]. These models are valued for their mathematical simplicity and effectiveness in environments with stable and predictable patterns. In particular, they tend to perform reasonably well in short-term forecasting scenarios. However, their inherent limitations become evident when applied to the highly dynamic and complex nature of modern cellular networks. Real-world traffic patterns are often nonlinear, influenced by diverse user behaviors, mobility patterns, and spatial interdependencies between network nodes. Linear models, by design, are not well suited to represent such complexity. Their reliance on assumptions of stable statistical properties over time and their limited capacity to model long-range or spatial correlations result in reduced predictive accuracy and reliability, particularly in long-term forecasting tasks. Consequently, while these methods remain useful in controlled settings, their applicability to large-scale, real-world networks is significantly constrained.

The continuous growth of network traffic, along with recent developments in ML, has led to increased interest in data-driven approaches for cellular traffic prediction. These methods are viewed as promising alternatives to traditional statistical models, particularly in handling the complexity and variability of modern network environments. However, simpler ML algorithms such as linear regression and support vector regression, often fall short. Their limited capacity to capture nonlinear and high-dimensional patterns makes them less suitable for accurate forecasting in real-world scenarios.

To overcome these limitations, researchers have increasingly adopted advanced DL architectures such as Long Short-Term Memory (LSTM) and Gated Recurrent Unit (GRU), which are specifically designed to handle long-term dependencies. These

models have been widely used for cellular traffic prediction due to their ability to learn from large volumes of sequential data [9], [10], [11]. For example, an LSTM-based traffic prediction model utilizing real-world call data is proposed in [12], demonstrating its ability to learn meaningful patterns in practical scenarios. Similarly, in [13], an LSTM model is used to predict a retainability Key Performance Indicator (KPI) from Ericsson's Long-Term Evolution (LTE) network in Algeria. On the other hand, GRUs, which offer a more computationally efficient alternative to LSTMs, have also been explored for similar applications [14]. Additionally, [15] proposes a GRU-based neural network model that predicts base station traffic by capturing the periodicity and fluctuating characteristics inherent in base station traffic data. Moreover, hybrid models that integrate LSTM or GRU with Convolutional Neural Networks (CNNs) have shown potential for improved feature extraction, though they come with added complexity and computational overhead [16], [17].

In general, recurrent models such as LSTM and GRU are considered excellent choices when it comes to modeling sequential patterns in cellular traffic data; however, their way of representing and leveraging any time-related information is limited. Standard approaches make use of static features for time representation, such as hour-of-day or cyclical encodings of time-not nearly sufficient to capture the richness of temporal patterns, such as long-term seasonal trends or the subtle finesse of daily and weekly cycles or demand surges at certain hours. The absence of a trainable expressive time representation renders a model incapable of adapting to non-stationary and multi-scale traffic dynamics.

3. Methodology

This section outlines the components of the proposed Time2Vec-enhanced LSTM model, including the Time2Vec encoding technique, the LSTM architecture, integration of Time2Vec, and the model's input-output structure, along with the training approach.

3.1. Time2Vec Embedding

Time2Vec is a time-encoding method that effectively incorporates temporal data into ML models. Rather than requiring manual construction of time-based features, Time2Vec learns a representation that includes long-term trends and recurring patterns in time-series data [18], [19]. Such an approach is very helpful in traffic prediction tasks, where time-dependent behaviors are either periodic (daily, weekly, etc.) or changing across time. For every scalar input t, Time2Vec produces a vector of size $k+1$, where the first component defines a linear transformation of time (modeling aperiodic trends), whereas the remaining k components model periodic variations in time using sinusoidal functions with trainable parameters for frequency and phase. This empowers Time2Vec to learn some of the complex time-related dynamics that are necessary in various real applications.

The Time2Vec function is mathematically expressed as Eq. (1):

$$Time2Vec = \begin{cases} \omega_0 \cdot t + b_0 & \text{if } i = 0 \\ \sin(\omega_i \cdot t + b_i) & \text{for } 1 \le i \le k \end{cases} \quad (1)$$

where ω_i and b_i are trainable weights and biases. The linear component $\omega_0 \cdot t + b_0$ captures long-term, non-periodic trends, while the sinusoidal components $\sin(\omega_i \cdot t + b_i)$ model periodic behaviors such as daily or weekly cycles.

3.2. LSTM Architecture Overview

LSTM is a type of Recurrent Neural Network (RNN) aimed at addressing the limits of traditional RNNs in modeling long-range dependencies within sequential data. This enables LSTM to excel in time series forecasting by retaining memory for long time intervals and avoiding issues such as vanishing gradients. The LSTM architecture consists mainly of four key components: the memory cell, the forget gate, the input gate, and the output gate, as illustrated in Fig. 1. The memory cell is a unit maintaining information and allows information to be continuously fed into following time steps, while the gates regulate what to allow in or out of the memory cell and what should be forgotten.

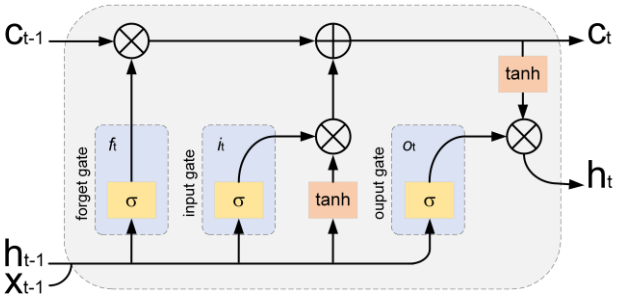

Fig. 1: LSTM cell structure showing the forget, input, and output gates, and the update of cell and hidden states

The forget gate is defined as Eq. (2):

$$f_t = \sigma\left(\omega_f [h_{t-1}, x_t] + b_f\right) \quad (2)$$

where $\sigma(\cdot)$ is the sigmoid function, x_t and h_{t-1} are the input and previous hidden state, and ω_f and b_f denote weight and bias parameters.

The activation output of Eq. (2) is bounded within the interval [0,1], with boundary values serving as binary gating signals. A null output (0) induces complete suppression of the preceding information, whereas unit output (1) facilitates perfect propagation through the temporal pathway. Subsequent to this gating operation, the system computes the state modification terms through two parallel transformations: (i) a sigmoidal regulatory layer (denoted as the input gate) that performs multiplicative modulation of the input stream, and (ii) a hyperbolic tangent transformation layer that generates a complementary candidate state vector. These components collectively implement the adaptive state update mechanism characteristic of LSTM architectures.

The input gate activation and the candidate value generation are defined as Eq. (3) and Eq. (4):

$$i_t = \sigma(\omega_i[h_{t-1}, x_t] + b_i) \quad (3)$$

$$c_t = f_t * c_{t-1} + i_t * \tilde{c}_t \quad (4)$$

where i_t denotes the activation of the input gate and $\tilde{c}_t$ refers to the vector of the new candidate values. By integrating these components, the updated cell state c_t is derived through the combination of Eq. (3) and Eq. (4), as expressed in Eq. (5):

$$c_t = f_t * c_{t-1} + i_t * \tilde{c}_t \quad (5)$$

The final step involves generating the output. A sigmoid activation is first applied to determine which components of the cell state should influence the hidden state. The updated cell state is then transformed using a hyperbolic tangent function to constrain its values within the range $[-1, 1]$, and this result is scaled by the output gate's activation to produce the final hidden state.

Eq. (6) and Eq. (7) formalize this process, where Eq. (6) computes the output gate activation, and Eq. (7) derives the updated hidden state based on the modulated cell state.

$$o_t = \sigma(\omega_o[h_{t-1}, x_t] + b_o) \quad (6)$$

$$h_t = o_t * \tanh(c_t) \quad (7)$$

where o_t denotes the output gate activation obtained from the sigmoid function, and h_t represents the resulting hidden state. This hidden state is subsequently passed to the next time step or network layer, enabling the model to maintain temporal context across sequences.

3.3. Proposed Time2Vec-Enhanced LSTM Model

To effectively capture complex temporal dependencies in mobile traffic data, we integrate the Time2Vec mechanism with an LSTM architecture as illustrated in Fig. 2.

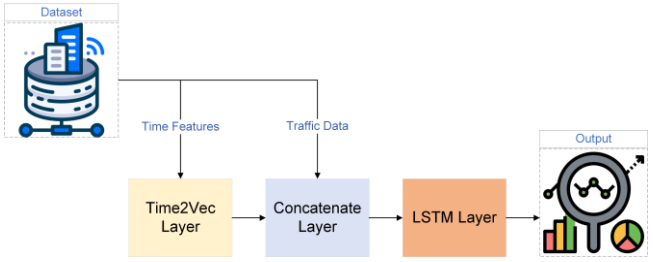

Fig. 2: The proposed hybrid Time2Vec-enhanced LSTM model

Traditional time encoding methods, such as one-hot or cyclical features, often fail to capture subtle periodic patterns, particularly when dealing with multiscale temporal trends. Time2Vec, a trainable time encoding function, addresses this limitation by learning both linear and periodic components of time explicitly, thereby improving the temporal awareness of the model.

3.3.1. Temporal Feature Extraction

In our architecture, raw temporal features such as hour of the day and day of the month, are first extracted from the timestamp. These temporal features are represented as a vector:

$$T = [Hour(t), Day(t)] \in \mathbb{R}^{d_t} \quad (8)$$

where T is a vector containing the extracted temporal features for each time step t, and d_t represents the dimensionality of the temporal feature vector.

These raw temporal features are then passed through a custom Time2Vec layer, which transforms them into a continuous vector representation. The Time2Vec layer outputs a concatenation of a linear transformation and several sine activations, allowing the model to capture both long-term linear trends and periodic cycles.

At each time step τ, the Time2Vec layer produces an embedding by combining a linear component and multiple periodic components as Eq. (9) below:

$$Time2Vec(T_\tau) = \begin{cases} \omega_0 \cdot T_\tau + b_0 & \text{if } i = 0 \\ \sin(\omega_i \cdot T_\tau + b_i) & \text{for } 1 \le i \le k \end{cases} \quad (9)$$

where ω_0 and b_0 are learnable scalar weights for the linear term, ω_i and $b_i \in \mathbb{R}^{d_t}$ are learnable parameters for the ith periodic function, with $1 \le i \le k$, and T_τ is the temporal feature vector at time step τ. This allows the model to learn both short-term cycles (e.g., hourly and daily) and long-term trends (e.g., variations over multiple days).

3.3.2. Feature Normalization

To ensure that all input features contribute proportionally to model training, we apply z-score normalization to both the traffic volume and temporal features before sequence modeling. This standardization process transforms each feature by subtracting the mean and dividing by the standard deviation, as defined in Eq. (10). It centers the data around zero with unit variance, which helps stabilize training and accelerates convergence of the LSTM model.

$$z = \frac{x - \mu}{\sigma} \quad (10)$$

where x is the raw feature value, μ is the mean, and σ is the standard deviation of the feature.

3.3.3. Model Input Structure

Let the normalized historical traffic features at time step τ be represented as Eq. (11) below:

$$x_\tau = [u_\tau, \Delta_\tau, \Sigma_\tau] \in \mathbb{R}^3 \quad (11)$$

where u_τ, Δ_τ, and Σ_τ denote the uplink, downlink, and total traffic volumes, respectively. Let $T_\tau \in \mathbb{R}^3$ denote the temporal feature vector at time step τ, which includes hour and day.

To incorporate recurring temporal patterns, we apply the

Time2Vec embedding $\phi(T_\tau) \in \mathbb{R}^{k+1}$ as defined in Eq. (9). We then concatenate the traffic vector x_τ with the temporal embedding to form the combined input defined as Eq. (12) below:

$$z_\tau = [x_\tau \parallel \phi(T_\tau)] \in \mathbb{R}^{3+k+1} \quad (12)$$

Over a sliding window of length L, we construct the input sequence as Eq. (13):

$$Z = [z_{\tau-L+1}, \dots, z_\tau] \in \mathbb{R}^{3+k+1} \quad (13)$$

This sequence is then passed into an LSTM layer, which models temporal dependencies in both traffic and time-aware patterns and is defined as Eq. (14):

$$h = LSTM(Z) \quad (14)$$

The LSTM output h is finally used to predict the traffic volumes at the next time step through a fully connected layer.

3.3.4. Output and Training Strategy

The final hidden state output from the LSTM, denoted as $h \in \mathbb{R}^d$, is passed through a fully connected (dense) layer to generate the predicted traffic volumes at the next time step:

$$\hat{y}_{\tau+1} = W_{out} \cdot h + b_{out} \quad (15)$$

where $W_{out} \in \mathbb{R}^{3\times d}$ is the learnable weight matrix projecting the LSTM hidden state $h \in \mathbb{R}^d$ to the output space, and $b_{out} \in \mathbb{R}^3$ is the learnable bias vector. The resulting prediction $\hat{y}_{\tau+1} = [\hat{u}_\tau, \hat{\Delta}_\tau, \hat{\Sigma}_\tau]$ corresponds to the uplink, downlink, and total traffic volumes at the next time step.

4. Dataset and Experimental Setup

4.1. Dataset Description

The dataset used in this study was collected from a telecom service provider operating in Kandahar Province, Afghanistan, and contains traffic data for an LTE base station with three cells. The data spans the entire month of November 2024, from November 1 to November 30, with continuous recording for 24 hours each day.

The dataset includes parameters such as Date and Time, Cell ID (which specifies one of the three cells), Uplink Traffic Volume (a measurement of data uploaded by users within a cell), Downlink Traffic Volume (a measurement of data downloaded by users within a cell), and Total Traffic Volume (the sum of uplink and downlink traffic, representing overall data consumption within each cell).

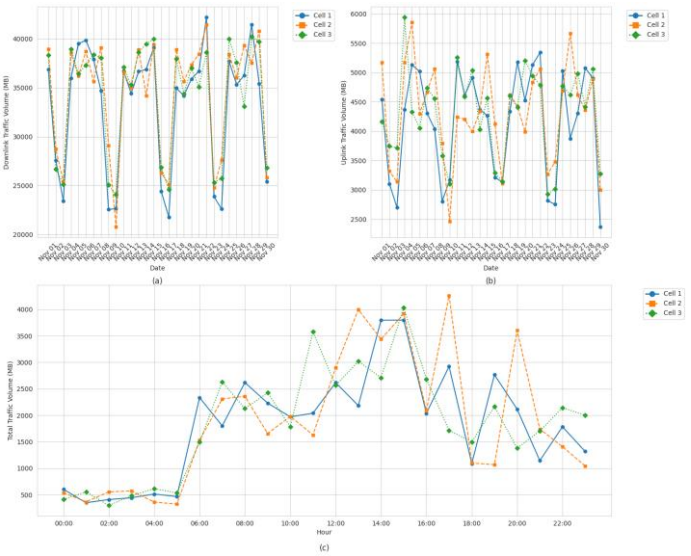

Fig. 3: Traffic volume analysis: (a) Daily Download Traffic Volume per cell, (b) Daily Upload Traffic Volume per cell, and (c) Hourly Total Traffic Volume per cell (November 15, 2024).

The dataset comprises a total of 2,160 samples, corresponding to hourly measurements collected across all three cells over the 30-day period. Different views of the dataset are shown in Fig. 3, and a summary of the descriptive statistics for these traffic parameters is provided in Table 1.

Table 1. Summary statistics of the dataset

Traffic Type	Minimum (MB)	Maximum (MB)	Mean (MB)	Standard Deviation (MB)
Uplink	11.39	800.50	177.09	132.81
Downlink	153.84	5,120.32	1,408.95	937.84
Total	173.9	5,920.82	1,586.04	1,037.09

4.2. Data Preprocessing

4.2.1. Train-Test Split

The dataset was split randomly into training and testing portions to enable the validation of the actual performance of the model and its ability to generalize over unseen data, as shown in Table 2. Special consideration was made to set aside 20% of the records as a test set, so that the model could be trained with 80% of the data. This kind of division is employed in real applications where a model is trained on historical data, then deployed to predict on future or unseen data. This random partition confines the elements present in both partitions to similar distributions and hence opposes the possibility of overfitting, giving a strong validation of the model.

Table 2. Train-test split of total traffic data

Feature	Total Samples	Training Set (80%)	Testing Set (20%)
Uplink Traffic	2160	1728	432
Downlink Traffic	2160	1728	432
Total Traffic	2160	1728	432

4.2.2. Feature Selection

From the raw dataset, we select two groups of features for modeling:

- Traffic-related features: uplink traffic volume, downlink traffic volume, and total traffic volume per hour.
- Temporal context features: hour of the day and day of the month, derived from the timestamp.

Traffic characteristics indicate the system's load level at each time, whereas temporal features provide the contextual setting for recurring patterns. The temporal features are fed into a Time2Vec embedding layer (discussed in Section 3) to encode linear as well as periodic time trends.

To ensure that all features contribute proportionally to the learning process, they are normalized using z-score standardization, as discussed in Section 3.3.2. We chose z-score over alternatives like min-max [20], as it better preserves variability and handles outliers, providing more stable inputs for the proposed model.

4.3. Evaluation Metrics

To evaluate the performance of the proposed Time2Vec-enhanced LSTM model for cellular traffic prediction, two commonly used evaluation metrics, namely RMSE and R^2, are employed. RMSE measures the average magnitude of the prediction error, while the R^2 describes exactly how much of the variance in the true data is explained by the model. Both predictive accuracy and explanatory power are incorporated into our evaluation using these metrics.

4.3.1. Root Mean Square Error (RMSE)

The RMSE represents the square root of the mean of squared deviation between forecasted traffic volume and actual observed traffic volume as described in Eq. (16). It is expressed with the same units as those of the observed traffic values (MB). So, the lower the RMSE values, the higher are the accuracies of the predicted values.

$$RMSE = \sqrt{\frac{1}{n}\sum_{i=1}^{n}(\hat{y}_i - y_i)^2} \tag{16}$$

where y represents actual target value, $\hat{y}$ denotes the predicted value, and n is the total number of observations.

4.3.2. Coefficient of Determination (R^2)

R^2 evaluates how well the variations existing in the actual traffic data are explained by the model. R^2 does possess values close to 1 when the model is able to capture the temporal patterns well, and the values approach 0 when the explanatory power is limited. R^2 is expressed in Eq. (17) as shown below:

$$R^2 = 1 - \frac{\sum_{i=1}^{n}(y_i - \hat{y}_i)^2}{\sum_{i=1}^{n}(y_i - \bar{y}_i)^2} \tag{17}$$

where $\bar{y}$ represents the mean of actual target values.

5. Results and Discussion

To evaluate the effectiveness of the proposed Time2Vec-enhanced LSTM model, experiments were conducted on a dataset comprising hourly cellular traffic data collected over a 30-day period as discussed in Section 4.1. The model was designed to forecast three target variables: uplink, downlink, and total traffic volumes, using both historical traffic patterns and temporal contextual features.

The Time2Vec layer was applied to the two available time-related features, hour and day, before concatenation with the traffic volume sequences. This temporal embedding captures both linear and periodic dependencies, which are crucial for modeling daily patterns and hourly fluctuations commonly observed in network traffic data.

5.1. Overall Performance Comparison

The predicted and actual traffic values for all three targets are visually compared in Fig. 4. The plots indicate that the predicted values closely follow the overall trends and periodic fluctuations of the true values, particularly for total traffic, where the model captures both sharp peaks and troughs effectively. Although some discrepancies are visible, the alignment between actual and predicted patterns supports the suitability of Time2Vec for encoding periodic temporal signals.

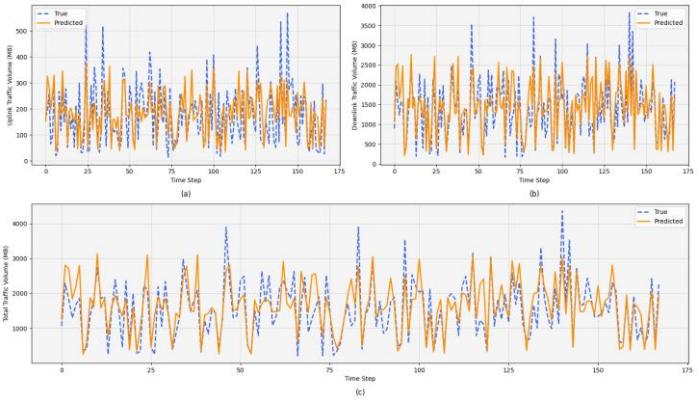

Fig. 4: Comparison of actual and predicted traffic volumes for (a) Uplink, (b) Downlink, and (c) Total Traffic over 175 time steps

Among the considered methods, the DL approaches (LSTM and GRU) demonstrated better performance than the traditional statistical and ML models, ARIMA and SVR, respectively,

particularly in terms of R^2 scores for downlink and total traffic. However, both LSTM and GRU still fell short of the performance achieved by the proposed model, which achieved the highest R^2 across all traffic types.

Table 3. Performance comparison of different models

Model	Traffic Type	RMSE (MB)	R^2 Score
Time2Vec-enhanced LSTM	Uplink	73.48	0.5991
	Downlink	468.52	0.6254
	Total	498.53	0.6531
LSTM	Uplink	92.25	0.3686
	Downlink	501.35	0.5711
	Total	539.62	0.5936
GRU	Uplink	94.78	0.3335
	Downlink	524.96	0.5298
	Total	547.22	0.5820
ARIMA	Uplink	103.10	0.3800
	Downlink	576.54	0.5333
	Total	604.65	0.5820
SVR	Uplink	108.81	0.1216
	Downlink	737.66	0.0308
	Total	828.70	0.0415
RF	Uplink	95.53	0.3228
	Downlink	533.93	0.5136
	Total	541.50	0.5907

The performance of the proposed Time2Vec-enahanced LSTM model was evaluated using RMSE and R^2 metrics and benchmarked against a diverse set of models, including LSTM, GRU, ARIMA, SVR, and RF. As illustrated in Table 3, the proposed model showed the best prediction accuracy with the least RMSE and maximum R^2, for all traffic types (uplink, downlink, and total), thus convincingly speaking for a better capturing of the temporal dynamics from cellular traffic data.

While ARIMA showed slightly better R^2 than GRU in the uplink case, its overall RMSE values remained higher. SVR performed the poorest across all metrics, with the highest RMSE and the lowest R^2 scores. The RF, meanwhile, produced mixed results. Its RMSE values were higher than those of LSTM and only marginally better than GRU for total traffic. Its R^2 scores generally lagged behind LSTM and GRU, however, for total traffic, its R^2 was slightly better than that of GRU. Despite having better performance comparing to ARIMA and SVR, it still showed slightly worse R^2 than ARIMA in the uplink and downlink cases. This indicates that although RF sometimes reduced average prediction error slightly compared to the weaker models, it struggled to capture the temporal patterns and variability in the data, often regressing toward the mean and failing under conditions of high fluctuation.

This set of results justifies the integration of learning temporal embeddings through Time2Vec into LSTM for further spatiotemporal modeling of cellular traffic. To provide a clearer comparison of performance, Fig. 5 visualizes the R^2 scores across all models for each traffic type, highlighting the consistent superiority of the proposed Time2Vec-enhanced LSTM model. It presents a grouped bar chart of R^2 values, with separate bars for uplink, downlink, and total traffic types across all evaluated models.

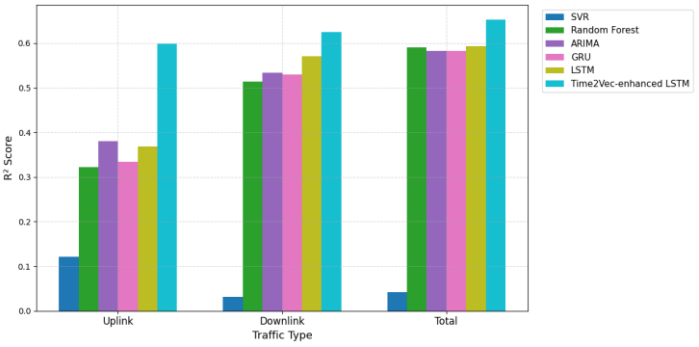

Fig. 5: R^2 scores of all considered models across traffic types

5.2. Ablation Study on Temporal Encoding

To better understand the impact of temporal feature encoding on model performance, an ablation study was conducted by comparing four LSTM-based architectures:

1) LSTM model using only traffic data (no time features),
2) LSTM with raw time inputs (hour and day),
3) LSTM with fixed cyclical encodings (sin/cos transformations),
4) the proposed Time2Vec-enhanced LSTM.

The performance differences among these models are illustrated in Fig. 6.

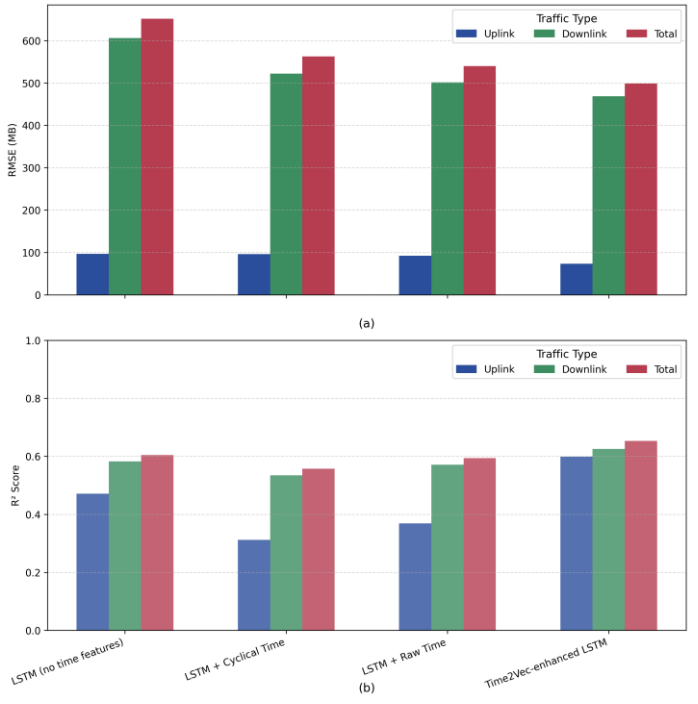

Fig. 6: Ablation study comparing (a) RMSE and (b) R^2 score across four LSTM-based models for uplink, downlink, and total traffic prediction

As shown in Fig. 6 (a) and (b), the inclusion and design of time features significantly affect the predictive performance. The LSTM with no time feature was found to have only moderate predictive capacity and is particularly limited in its ability to capture temporal dependencies inherent in the data. The inclusion of cyclical time encodings resulted in slightly reduced RMSE values for downlink and total traffic in comparison to the LSTM with no time feature, while it tended to have reduced R^2 scores for all traffic types. This would indicate that fixed periodic encodings do not properly capture the temporal variability in the data. On the other hand, LSTM with the raw hour and day features was better in some cases than the basic LSTM and its cyclical variants, indicating that whatever the model can glean from raw temporal inputs is worthwhile.

In contrast, the Time2Vec-enhanced LSTM consistently achieved the lowest RMSE and highest R^2 scores across all traffic types, clearly outperforming all other variants. These results confirm that learnable temporal embeddings from Time2Vec provide a more expressive and adaptive representation of time, enabling the model to better capture both short-term patterns and long-term periodic trends in the traffic data.

6. Conclusions

In this study, a hybrid Time2Vec-enahanced LSTM model was proposed for traffic volume prediction in cellular networks. The model simultaneously integrates periodic temporal features with historical traffic data so that independences of short-term changes and long-term cyclic patterns can be learned.

Experiments indicated that the proposed Time2Vec-enhanced LSTM model is dominant compared to considered DL, time series, and ML methods for uplink, downlink, and total traffic volume prediction. The model achieved lower RMSE and higher R^2 scores across all traffic types, consistently outperforming all the models. Additionally, the ablation study confirmed that the Time2Vec-based temporal encoding was the key factor driving this superior performance, as models without time features or using only raw or cyclical time inputs consistently showed higher errors and lower R^2 scores. Its strong performance is attributed to the inclusion of learnable periodic transformations via Time2Vec, which significantly enhanced the LSTM's capacity to recognize cyclical patterns in the data.

Summing up, the findings corroborate the importance of temporal embeddings in DL-based traffic prediction. The proposed Time2Vec-enhanced LSTM architecture appears to be a potential candidate for intelligent network traffic prediction.

In the future, research may be undertaken to extend the model to multi-cell scenarios and to experiment with more time features such as weekends, holidays, and special events, while hyperparameter tuning could be applied to achieve improved prediction accuracy and performance.

References

[1] J. Xiao, Y. Cong, W. Zhang, and W. Weng, "A cellular traffic prediction method based on diffusion convolutional GRU and multi-head attention mechanism," *Cluster Computing*, vol. 28, no. 2, p. 125, 2025.

[2] H. Riaz, S. Öztürk, and A. Çalhan, "A Robust Handover Optimization Based on Velocity-Aware Fuzzy Logic in 5G Ultra-Dense Small Cell HetNets," *Electronics*, vol. 13, no. 17, Art. no. 17, Jan. 2024, doi: 10.3390/electronics13173349.

[3] H. Riaz, S. Öztürk, S. Aldirmaz-Colak, and A. Çalhan, "A Handover Decision Optimization Method Based on Data-Driven MLP in 5G Ultra-Dense Small Cell HetNets," *J Netw Syst Manage*, vol. 33, no. 2, p. 31, Feb. 2025, doi: 10.1007/s10922-025-09903-6.

[4] O. Aouedi, V. A. Le, K. Piamrat, and Y. Ji, "Deep Learning on Network Traffic Prediction: Recent Advances, Analysis, and Future Directions," *ACM Comput. Surv.*, vol. 57, no. 6, p. 151:1-151:37, Feb. 2025, doi: 10.1145/3703447.

[5] X. Wang *et al.*, "A Survey on Deep Learning for Cellular Traffic Prediction," *Intelligent Computing*, vol. 3, p. 0054, Jan. 2024, doi: 10.34133/icomputing.0054.

[6] H. Riaz, P. Güneş, H. Benli, and F. H. Ahmadzai, "A Comparative Analysis of Machine Learning Models for Cellular Load Prediction: Insights from Real-World Data," *Journal of Emerging Trends in Engineering Research*, vol. 13, no. 4, pp. 73–81, 2025.

[7] A. Azari, P. Papapetrou, S. Denic, and G. Peters, "Cellular traffic prediction and classification: A comparative evaluation of LSTM and ARIMA," presented at the Discovery Science: 22nd International Conference, DS 2019, Split, Croatia, October 28–30, 2019, Proceedings 22, Springer, 2019, pp. 129–144.

[8] S. Medhn, B. Seifu, A. Salem, and D. Hailemariam, "Mobile data traffic forecasting in UMTS networks based on SARIMA model: The case of Addis Ababa, Ethiopia," presented at the 2017 IEEE AFRICON, IEEE, 2017, pp. 285–290.

[9] X. Cao, Y. Zhong, Y. Zhou, J. Wang, C. Zhu, and W. Zhang, "Interactive Temporal Recurrent Convolution Network for Traffic Prediction in Data Centers," *IEEE Access*, vol. 6, pp. 5276–5289, 2018, doi: 10.1109/ACCESS.2017.2787696.

[10] C. Zhang, H. Zhang, J. Qiao, D. Yuan, and M. Zhang, "Deep Transfer Learning for Intelligent Cellular Traffic Prediction Based on Cross-Domain Big Data," *IEEE Journal on Selected Areas in Communications*, vol. 37, no. 6, pp. 1389–1401, Jun. 2019, doi: 10.1109/JSAC.2019.2904363.

[11] C. Gijón, M. Toril, S. Luna-Ramírez, M. L. Marí-Altozano, and J. M. Ruiz-Avilés, "Long-Term Data Traffic Forecasting for Network Dimensioning in LTE with Short Time Series," *Electronics*, vol. 10, no. 10, Art. no. 10, Jan. 2021, doi: 10.3390/electronics10101151.

[12] S. Jaffry and S. F. Hasan, "Cellular traffic prediction using recurrent neural networks," presented at the 2020 IEEE 5th international symposium on telecommunication technologies (ISTT), IEEE, 2020, pp. 94–98.

[13] H. Chekireb, L. Fergani, S. A. Selouani, M. R. Deramchi, and R. Rochedi, "Improving LTE network Retainability KPI prediction performance using LSTM and Data Filtering technique," presented at the 2022 7th International Conference on Image and Signal Processing and their Applications (ISPA), IEEE, 2022, pp. 1–6.

[14] W. Jiang, M. He, and W. Gu, "Internet Traffic Prediction with Distributed Multi-Agent Learning," *Applied System Innovation*, vol. 5, no. 6, Art. no. 6, Dec. 2022, doi: 10.3390/asi5060121.

[15] T. Xu and Y. Yan, "Cell base station traffic prediction based on GRU," *Comput. Perform. Commun. Syst*, vol. 7, no. 1, pp. 66–72, 2023.

[16] K. Gao *et al.*, "Predicting Traffic Demand Matrix by Considering Inter-flow Correlations," in *IEEE INFOCOM 2020 - IEEE Conference on Computer Communications Workshops (INFOCOM WKSHPS)*, Jul. 2020, pp. 165–170. doi: 10.1109/INFOCOMWKSHPS50562.2020.9163001.

[17] D. Aloraifan, I. Ahmad, and E. Alrashed, "Deep learning based network traffic matrix prediction," *International Journal of Intelligent Networks*, vol. 2, pp. 46–56, Jan. 2021, doi: 10.1016/j.ijin.2021.06.002.

[18] S. M. Kazemi *et al.*, "Time2vec: Learning a vector representation of time," *arXiv preprint arXiv:1907.05321*, 2019.

[19] K. Zhou, C. Zhang, B. Xu, J. Huang, C. Li, and Y. Pei, "TE-LSTM: A Prediction Model for Temperature Based on Multivariate Time Series Data," *Remote Sensing*, vol. 16, no. 19, Art. no. 19, Jan. 2024, doi: 10.3390/rs16193666.

[20] H. Riaz, S. Öztürk, S. A. Çolak, and A. Çalhan, "Performance Analysis of Weighting Methods for Handover Decision in HetNets," *Gazi University Journal of Science*, vol. 37, no. 4, pp. 1791–1810, Jan. 2024, doi: 10.35378/gujs.1373452.

A Systematic Review of Laser Surfacing, Resurfacing, and Cutting

Akpaduado John*, Nick Caiazzo**, and Tom Griese***

* Ph.D. Student, Department of Mechanical Engineering and Mechanics, P.C. Rossin College of Engineering and Applied Sciences, Lehigh University, 27 Memorial Drive West, Bethlehem, PA, USA.

E-mail: afj223@lehigh.edu ORCID: 0000-0002-8220-7093

** Master's Student, Department of Mechanical Engineering and Mechanics, P.C. Rossin College of Engineering and Applied Sciences, Lehigh University, PA, USA.

E-mail: nickcaiazzo8@gmail.com ORCID: 0009-0004-7794-5405

*** Master's Student, Department of Mechanical Engineering and Mechanics, P.C. Rossin College of Engineering and Applied Sciences, Lehigh University, PA, USA.

E-mail: tog224@lehigh.edu ORCID: 0009-0009-7135-5638

Corresponding Author: Akpaduado John, Lehigh University, Bethlehem, PA, USA

Received: 26.05.2025 Accepted: 08.08.2025

Abstract- Laser surfacing, resurfacing, and cutting are leading-edge laser machining processes that bring benefits not previously known to the machining industry through state-of-the-art techniques. Laser machining is growing rapidly as the industry adopts additive manufacturing, creating a need for a process review. This study aims to critique the viability of laser surfacing, rust removal, and cutting machine processes in industry. A comprehensive literature review approach was adopted on previous studies on laser machining processes. The study also mirrored the effects of laser machining operations parameters by determining how changing them affects the final product. The results confirmed that laser surfacing can enhance surface finish on both simple and complex geometries for various materials. It was also discovered that thermal expansion and pressure waves can remove unwanted particles such as rust and dirt in the case of laser cleaning. Laser cutting provides a thorough and precise cut with no tool wear. These methods can efficiently and precisely perform across various complex geometries with little waste and no tool wear. Additionally, results show that laser power and scanning speed parameters are the most important laser parameters used in determining the success of a laser machining operation. Hence, the authors emphasized the importance of carefully selecting laser parameters, ensuring they are specifically tailored to the material and condition of the workpiece. They also advocated further research to optimize parameter selection in laser machining processes.

Keywords: Laser surface finishing, laser cutting, laser rust removal, scanning speed, laser power, pulsing frequency, gas pressure

1. Introduction

Surface finishing, resurfacing, and cutting are machining operations widely used in the fabrication and upkeep of metal parts. These processes are effective for most cases and especially useful for simple geometry parts. Downsides of current methods include a lack of flexibility in part geometry, time required to treat, and the necessity to replace tooling due to wear [1].

Surface finishing is a very significant area in the manufacturing of products in industries where surface properties are critical to the functionality of the final product. It is one of the standard quality metrics for most mechanical components. In the aerospace, medical, automotive, and electronics industries, surface finish is critical to the functionality, aesthetics, mechanical properties, topographic quality, and accuracy of products that have very stringent tolerances for proper operation. Current techniques used in the industry to achieve these include milling, abrasive methods, and chemical processes.

Resurfacing, sometimes referred to as cleaning, refers to the removal of contaminants on the surface layer of a part (usually rust/oxidation). Hence, the method can be applied to small parts that are refurbished and reused or to enlarge steel structures to extend life of such structures. Current methods include sandblasting, grinding, and chemical sprays. Major downsides are labor intensity and environmental sustainability [2].

Cutting is the oldest and most established method of the three being discussed and can be applied to a plethora of applications. Cutting can take the form of a cutoff tool on a lathe, milling to remove material, rotating or reciprocal saws in wood and metal, and table machine operations for sheet metal. In this paper, attention also focuses on the area of table machine cutting operations. Current table machine methods include waterjet and plasma cutting. Research affirmed that the major downside of waterjet cutting is its relatively slow cutting speed. The downside of plasma cutting is its relative lack of precision and rough-cut quality [3].

1.1 Concept of Laser Surface Finishing

Laser surface finishing leverages the precision and high energy density of lasers to induce localized re-melting to polish or ablate surface asperities and create a finish that is within quality control standards of a final product without any mechanical interaction **(Fig. 1).** These two methods utilize distinct underlying physical mechanisms to achieve the same premise of superior surface finish. However, works of literature on re-melt polishing as a technique of interest for achieving laser surface finishing were reviewed extensively in this study.

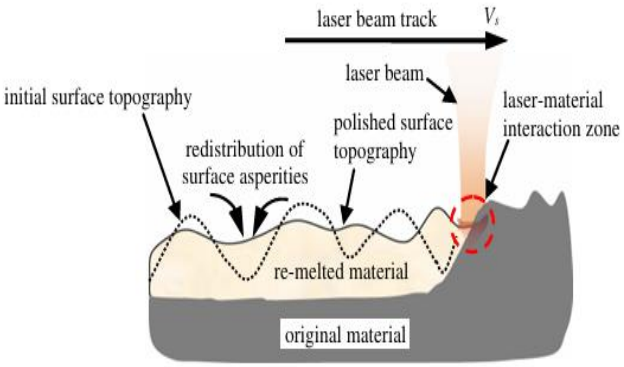

Fig. 1. Schematic of laser remelting mechanism [5]

Remelting is primarily governed by the nuanced physics of micro-melt pools created from laser energy deposition. B. Guan et al. [4] and Bordachev et al. [5] in their studies on the performance of laser polishing in finishing metallic surfaces. The studies elucidated the mechanism of a laser beam's operation. According to the study, the laser beams acting on the material surface have a near-Gaussian energy distribution, with central areas of effect hotter than the edges, inducing a temperature gradient in the area. The studies elucidated the mechanism of a laser beam's operation. According to the study, the laser beams acting on the material surface have a near-Gaussian energy distribution, with central areas of effect hotter than the edges, inducing a temperature gradient in the area. Based on the material reflectivity and absorption coefficient, the transient temperature field behaves according to the heat equation. When the melt temperature is reached, this flow of melted material is governed primarily by Marangoni convection, which drives cooler, more viscous, and more surface-tense liquid to flow towards hotter, less viscous, and surface-tense areas, inducing shear stresses in the fluid. This effect, combined with the principles of capillary pressures, induces normal stresses on the surface flow, driving flow from high areas of curvature, present on the convex surface peaks, to low areas of curvature on the surface valleys. Solidification typically occurs at cooling rates ranging from 10^3 to 10^6 K/s. The heat energy diffuses to the bulk material from the melt pool almost instantaneously because the immense temperature gradient is created, localized to the melt on the scale of only a few micrometers. This rapid solidification results in ultra-fine grain structures on these surfaces that are free of large crystallite growths, and are exceptionally harder than the underlying material, unaffected by the heat of polishing. This physical behavior, coupled with the thermal and fluid dynamical effects present, culminates in surfaces solidifying with smooth, homogenous topographies [4] and [5].

Laser remelting is advantageous over traditional surface finishing techniques in many ways for industrial applications. It is a non-contact, non-abrasive technique that essentially eliminates tool wear, contamination from consumables, and preserves underlying bulk material and its mechanical properties. Due to the inherent lack of tooling required, maintenance requirements and downtime can be minimized. Complex geometries, unlimited internal channels, and lattice structures are polished without a rigid mechanical fixture with a non-contact nature. Lasers can be mounted to CNCs or robotics and automated to treat the specific component being manufactured. The rapid heating and cooling inherent in the remelting process can create a surface layer that exhibits enhanced hardness, corrosion resistance, and mechanical wear resistance compared to surfaces left untreated during the manufacturing process. It applies to a wide array of metal alloys, ceramics, and glasses, provided parameterization is optimized for the desired laser-material interaction **(Fig. 2)**. Laser re-melting reduces environmental impacts by eliminating the need for hazardous corrosive chemicals and simplifying cleanups. Integration into additive manufacturing (AM) processes has an upside. Typically, these parts have surfaces that exhibit high roughness and unmelted particulates. By incorporating these methods into the manufacturing processes involved, manufacturing can be streamlined and potentially remove the errors present when relocating products to other facilities for treatment. The technologies of laser surface remelting present compelling upside to areas of manufacturing where high throughput, streamlined manufacturing, minimal material interaction, material versatility, and sustainability are paramount [5].

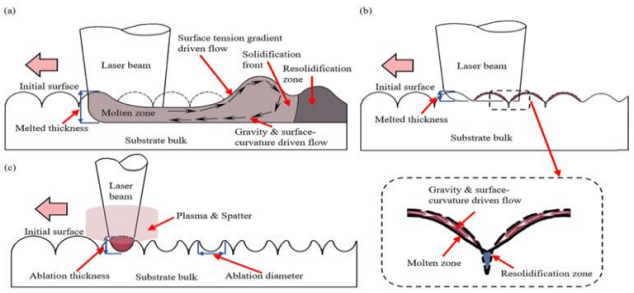

Fig. 2. Surface periodic waviness formation in (a) Surface over melting, (b) Shallow surface melting, (c) Laser surface ablation [4]

Investigations revealed that several barriers are impacting the widespread adoption of this technology. One of the many affirmed that it requires a very high upfront capital investment and operational costs. Secondly and perhaps most importantly, parameter optimization is non-trivial and requires significant research to optimize the large number of variables that are entirely process, material, and specific geometry. Empirical trials and numerical simulations are options, but they can be highly resource-intensive and costly to develop. In tandem, surface waviness can result from the governing melting mechanisms becoming unstable and oscillatory, which, paired with the fast-cooling rates, can lead to surfaces solidifying with periodic ripples. This can be a direct result of poorly optimized laser parameters leading to transient Marangoni forces. Self-excited capillary forces create capillary waves (ripples) along the phase boundary. These effects are highly driven by surface tension. When dealing with such sensitive microfluidic flows and localized precision. It can also be difficult to dampen external mechanical vibrations, which can create irregularities. Finally, the improvement and development of closed-loop feedback and sensor technologies for real-time enhanced control of processes are yet to come to full fruition. **Fig. 3** depicts the material cross-section hardening report due to laser polishing as published by Bordachev et al [5].

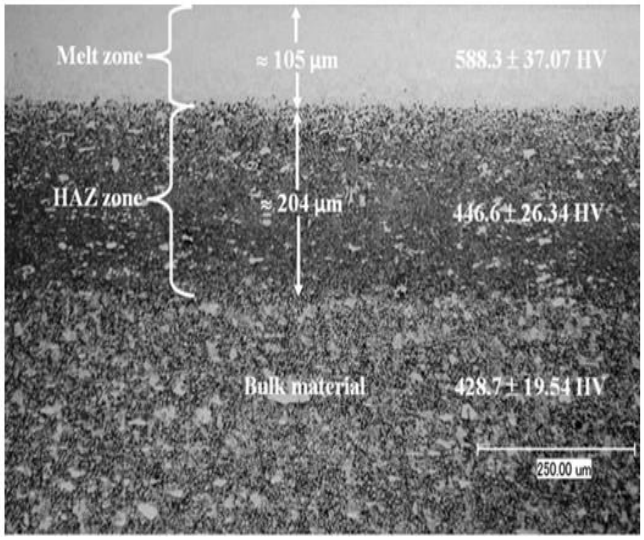

Fig. 3. Material cross-section hardening due to laser polishing [5]

1.2 Concept of Laser Resurfacing (Cleaning)

The laser resurfacing (cleaning) mechanism can be described by three submechanisms: surface irradiation, laser etching, and laser ablation [3]. While they are separate terms, the processes listed previously normally work in unison to create laser cleaning. The broader process of laser cleaning can be broken down into three main processes: dry laser cleaning, liquid-assisted laser cleaning, and laser shock wave cleaning [6]. Each of these methods uses similar yet different concepts to remove rust and dirt from surfaces. Unlike laser polishing, laser cleaning cannot fully rely on the melting and settling of the surface substrate to completely remove it. Rather, laser cleaning relies on the effects of pressure waves and expansion forces to impact the surface substrate, overcome any surface tension or van der Waals forces, and remove the substrate from the surface. Rust, dirt, and paint from surface substrates on structural steel components, as well as smaller parts that are

assigned for refurbishment, are removed using the laser resurfacing method. The cleaning method adopted, the Liquid-Assisted Laser Cleaning Mechanism, and the corresponding Shock Wave Cleaning by Zhu et al. [6] in 2022 are presented in Figs. 4, 5, and 6.

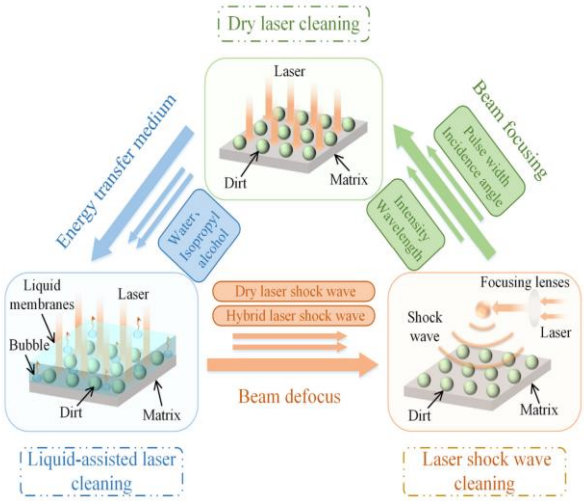

Fig. 4. Pulsed laser cleaning methods [6]

Dry laser cleaning is one of the most widely used methods. This method involves direct laser irradiation of the surface by focusing the laser beam on a specific area on the workpiece. The surface substrate and particles (usually paint or rust) absorb the laser beam's energy through a few mechanisms, and the unwanted particles are eventually dispersed from the surface once a high enough energy level is absorbed. These mechanisms include previously mentioned terms such as ablation and etching, where part of the substrate is vaporized as other parts are heated up enough to a point where the thermal expansion in the material causes them to detach from the surface they were bonded to [7] and [8]. Dry laser cleaning is free from liquid surface coating to help the cleaning process. Laser parameters such as power and pulse frequency determine how well a given surface is cleaned. Optimization and selection of these parameters will be discussed in further sections of this paper.

Literature also revealed that liquid-assisted laser cleaning, such as dry laser cleaning, can be performed with the additional step of adding a thin film of liquid to the surface. The necessity of adding this film of liquid is to reduce the possibility and effects of overheating of the base metal surface, which can occur in dry laser cleaning, resulting in unwanted damage to the workpiece, as well as a possible increase in the rate of particle removal. In this method, the liquid film is overheated. This results in the vaporization of the fluid film. Rapid evaporation and bubble expansion of this liquid have been shown to increase the magnitude of pressure waves produced by the laser, resulting in a more effective ejection of unwanted surface particles than in the dry laser cleaning case [9]. If the heating rate is sufficient, explosive phase change and evaporation can occur, enough to detach surface particles [10].

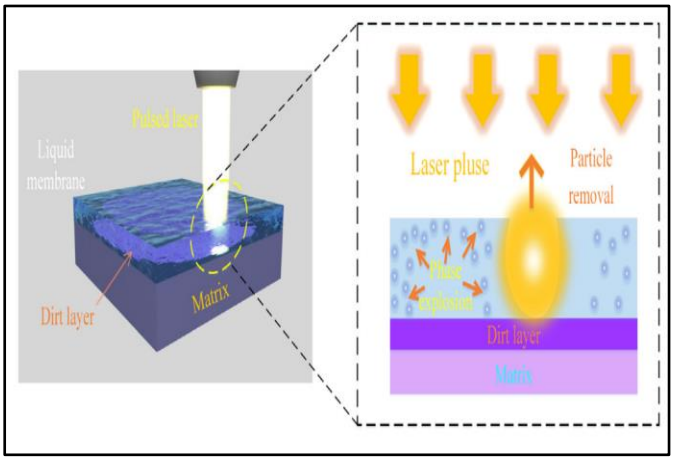

Fig. 5. Liquid-assisted laser cleaning mechanism [6]

Laser shock wave cleaning, as the name suggests, relies on miniature pressure (shock) waves that are formed by focusing the laser at a set distance above the work surface without direct laser impact on the surface. Through laser-induced breakdown of the ambient gas above the work surface, a strong enough shock is formed to remove small particles formed [11]. This method is not commonly used in rust removal, where particles are relatively large and bonded to the surface. However, it is useful in delicate situations where protection of the base workpiece is required.

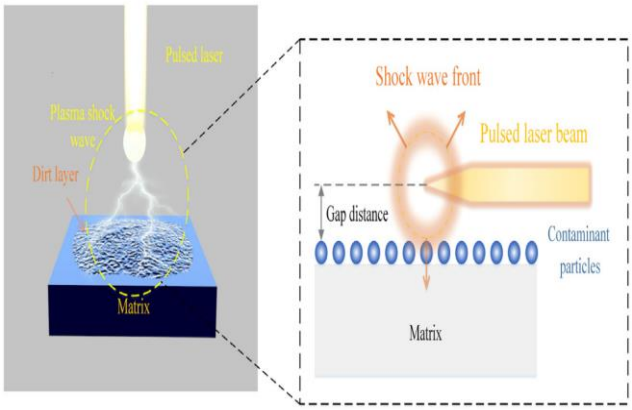

Fig. 6. Laser shock wave cleaning [6]

The preceding paragraphs laid some groundwork for how laser cleaning is applied to surfaces with larger contaminants, such as rust, as well as to smaller particles on delicate substrates. In the following sections of this paper, we will further explore how laser parameters are selected for the effective removal of surface materials. The focus will be on the dry laser cleaning method, as it is the most widely used and has proven effective for rust removal.

1.3 Concept of Cutting Techniques

The cutting process is one of the most advanced machining processes. It is often used with CNC software in sheet metal fabrication settings, where large quantities of sheet metal are cut before being fabricated. Using a laser beam focused on a small area on the workpiece, energy is absorbed by the work material. With this energy absorption, the material begins to heat up and eventually gets to a point where phase changes occur. The material melts and vaporizes, leaving behind a cut surface [12]. Laser cutting provides numerous advantages over other cutting methods, including minimal material removal, minimal distortion, and no tool wear [13].

There are a few parameters that should be observed in laser cutting, which determine how cut is left behind. Some of these parameters include surface roughness, kerf width, and heat-affected zone (HAZ) [14]. Surface roughness refers to the unevenness of the cut edge and cross-section and is undesirable in all applications. A better surface finish helps the fatigue life of the workpiece, and with a seamless editing or deburring of the cut material [15]. Kerf width is the width of the cut produced by the laser. The importance of this parameter can never be overemphasized in determining how well the geometric accuracy of the cut is. Lastly, the HAZ refers to the area around the cut where the material's microstructure changed, but the material did not melt [12]. The size of the HAZ determines how much of the material's physical properties changed after cutting [**Fig. 3**]. Changing physical properties can result in harder and more brittle material that is often unwanted, especially in processes where further machining is required. For example, plasma cutting is notorious for leaving a relatively large HAZ and a rough cut. This results in a harder material that can cause excessive wear on tooling used on the cut piece during machining [15]. Fig.7 shows the schematic explanation of the Kerf Width, HAZ, and Surface Roughness Illustration.

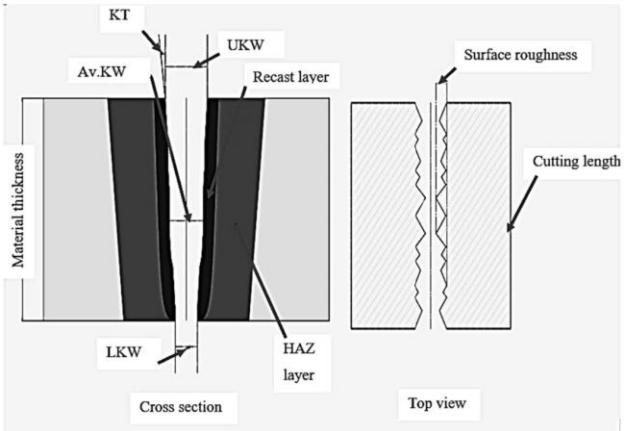

Fig. 7. Kerf width, HAZ, and surface roughness illustration [15]

2. Literature Review

Studies affirmed that laser surfacing, resurfacing (cleaning), and cutting enhance machining precision, efficiency, material performance, and surface integrity, optimizing manufacturing processes through reduced preparation time. Therefore, minimizing material waste and improving dimensional tolerances for engineering applications.

2.1 Laser Surface Finish Process

Laser surfacing represents a significant advancement in additive manufacturing, involving the sequential construction of material layers using a laser as the primary energy source. [8]. Dolgova et al. [16] analyzed deposition parameters for single laser tracks on austenitic steel 316L, identifying optimal conditions: 1,250 W laser power, 25 mm/s scanning speed, and ensuring precise geometric characteristics. Coatings containing iron, nickel, and tungsten carbide applied to 65 Mn steel samples enhance wear resistance. A schematic diagram of laser surfacing is shown in **Fig. 8**. Research affirmed that the abrasive resistance of a multicomponent charge with additives of 5 and 7 wt.% carbides are 2.45, 3.29, and 4 times higher than the base material of 65 Mn steel, Biryukov et al. [17] and Caggiano et al. [18]. When the propagation distance exceeded

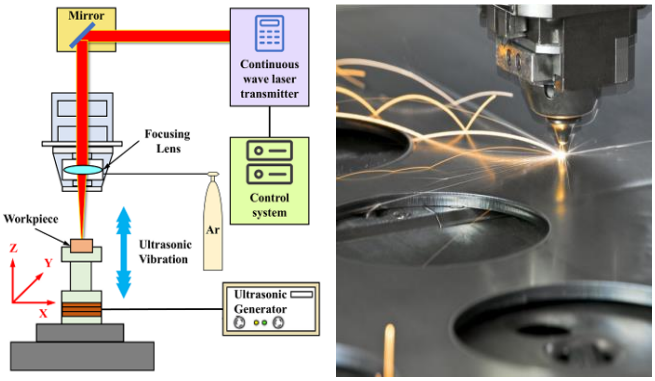

Fig. 8. Laser surface finishing schematic experimental setup [8] and *sgproto.com)*

10 mm, the defect signal in the acquired images displayed prominent noise points [19]. Laser polishing enhances surface quality, reduces roughness, improves density, and optimizes the mechanical properties of materials [20]. Abhishek et al. [21] and Caggiano et al. [18] applied innovative laser polishing with beam wobbling to Cr–Cu steel automotive parts. Results show that laser polishing enhances surface smoothness (62–78%) with limited microstructural changes using optimal wobbling parameters. Laser polishing significantly reduces surface roughness, enhances micro-hardness, and improves

specific properties of additively manufactured metals [22] and [23].

Additive manufacturing enables the creation of complex parts that traditional methods, such as machining or forging, cannot easily produce. Research highlighted that additive manufacturing parts require surface finishing to enhance quality and reduce the adverse effects of roughness [22] and [12]. Additive manufacturing (AM) is a dependable method for producing intricate and complex metallic components. Direct energy deposition (DED) is widely utilized in the production of metal alloys in additive manufacturing [4]. Vladimir proposed a laser surfacing technique that defocused and oscillated beams to charge particles suitable for testing 65 Mn coating steel for wear resistance. The results show that uniform coatings improve microhardness and enhance abrasive wear resistance significantly [18].

2.2 Laser Resurfacing (Cleaning) Process

Jing et al. [2] explored laser cleaning technology for isolator switches, analyzing principles and device design as a case study. Results show that optimal scanning speed and frequency improve cleaning efficiency and quality, providing effective rust removal without damaging the equipment base. Laser cleaning efficiently removes rust from steel surfaces while minimizing environmental impact. Optimal laser parameters prevent surface discoloration and do not affect material removal rate, showcasing its effectiveness and precision in industrial applications [24]. Narayanan et al. [25] and Gisario et al. [26] identified optimal laser parameters achieving material removal rates of 0.1–0.4 mm³/s with 90% accuracy. Maximum material removal occurred at 7.5–10 W, a hatch distance of 45–50 µm, a scanning speed of 875 mm/s, and a pulse repetition rate (PRR) of 50 kHz. The integration of response surface methodology with the second-generation non-dominated sorting genetic algorithm (NSGA-II) is a highly effective approach for optimizing laser cleaning parameters in rust removal applications [27]. Research demonstrates that optimal laser cleaning parameters include a laser power of 44.99 W, a cleaning speed of 174.01 mm/min, a scanning speed of 3852.03 mm/s, and a repetition frequency of 116 kHz. Zheng et al. [28] conducted a detailed investigation into the defocused nanosecond laser paint removal of mild steel substrates under atmospheric conditions, providing valuable insights for enhancing efficiency. Hence, reducing substrate damage in industrial applications. To safeguard steel bridges against corrosion, various advanced

rust removal techniques were established. Vinod et al. [1] conducted a critical review of corrosion development and rust removal in steel bridges. The Schematic description of the laser cleaning process is presented in **Fig. 9**. The results revealed that Laser cleaning effectively removes rust, minimizes steel damage, and is environmentally safe, but it incurs a high cost. Laser cleaning is an innovative and emerging approach with significant potential for industrial applications [29]. Laser cleaning machines with a power of 100 W or above can effectively perform precision cleaning, widely promoted in the field of power systems [30]. The amplitude and the local standard deviation of the acoustic signal in the frequency range of 7–10 kHz gradually decrease to a steady value in laser paint cleaning [4], [7], and [18].

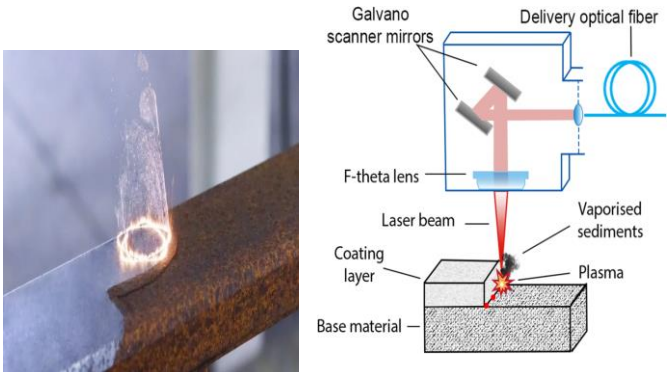

Fig. 9. Schematic description of the laser cleaning process [41], *sinbadlab.com.*

2.3 Industrial Cutting Techniques

Cutting technique is an industrial operation where a workpiece, such as metal, and the tool are moved over each other to shape the workpiece into the desired form through shaving, drilling, etc. The importance of cutting cannot be overemphasized. The techniques are highlighted among the advanced machining processes in modern manufacturing. They are frequently integrated with CNC software in sheet metal fabrication environments, facilitating the precise and efficient processing of large volumes of sheet metal before subsequent fabrication stages [5].

2.3.1 Laser Cutting Technique

Research affirmed that optimal laser cutting parameters achieve superior surface and kerf quality with reduced roughness and taper. Garcia-Fernandez et al. [31] investigated the impact of laser cutting parameters on the quality of cut surfaces and kerf. Using a comprehensive review of existing studies, analyzing performance through graphs, equations, and organized tables. Automation of tasks to replace manual processes, utilizing a control panel and ERP integration. Shortened production times, elimination of manual errors, and real-time updates on stock and production processes [32]. Ni et al. [33] examined the laser surface texturing (LST) of cutting

tools to enhance the machining of titanium alloys such as Ti6Al4V. The result shows that LST enhances cutting-tool tribological performance, reducing wear, friction, cutting forces, and temperatures. Deng et al. [34] and Ni et al. [33] reviewed LPBF progress for Ti–6Al–4V in aerospace, biomedical fields. Adopt process parameters and thermal effects on forming properties. The report affirmed machining improvements in cutting force, tool wear, and surface quality. Optimized cutting parameters for acrylic using CNC laser cutting by applying the Taguchi method to test laser power, speed, and focus, giving smoother cuts and improved efficiency with precise parameters [35]. Laser cutting can never be overemphasized. Laser cutting is widely used for accurate, non-contact cutting of metals and non-metallic materials. **Fig.10.** depicts a schematic diagram of a laser cutting technique.

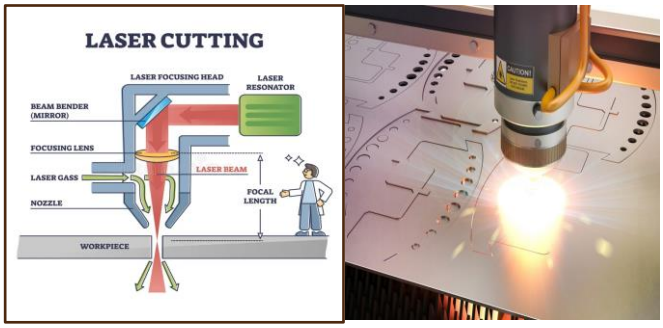

Fig. 10. Laser cutting techniques (Google.com and laserflow.com)

İrsel et al. [15] utilized a powered laser beam in laser beam cutting, plasma in plasma arc cutting, and a flammable gas-oxygen mixture in the oxygen cutting method to investigate the effects of various cutting methods and verify their advantages and disadvantages in cutting structural steels. It was discovered that plasma arc cutting increases hardness and reduces costs, while laser cutting provides superior precision and machinability. Naresh et al. [36] investigated the application of FEA, software nesting, and quality management to optimize the processing parameters: scanning speed, laser power, pulsing frequency, and gas pressure for laser cutting, minimizing equipment downtime caused by unnecessary stoppages.

2.3.2 Water Jet Cutting Technique

Krajca et al. [37] compared metal water jet cutting with laser and plasma cutting. The results show that water jet cutting proves to be the most versatile, eco-friendly, and effective for thick metal materials. The mechanical properties of the highly heat-sensitive acrylic can be considered by understanding the precise cutting process on a 40-watt CNC laser cutting machine. A water jet cutting technique utilizes thin water jets under high pressure with an abrasive slurry to cut the target material using erosion. It was patented in 1968 by a researcher in the USA, but developed rapidly in the 1980s. High-pressure water pumps are available in the range of 276 MPa to 689 MPa. This cutting method is common in the automobile industry, aerospace industry, construction engineering, chemical process engineering, environmental engineering, and industrial maintenance. Some of the leading companies are OMAX Corp. in Kent, Washington (largest), KMT Water System Inc., Kansas, WARD Jet Inc. in Ohio, Niche Inc., Massachusetts [37]. **Fig.11.** depicts a schematic diagram of a water-jet cutting technique.

Fig. 11. Water jet cutting technique (*Google.com and waterjet-cutting.com)*

2.3.3 Plasma Cutting Technique

A process that cuts through electrically conductive materials using an accelerated jet of hot plasma. This technology works by ionizing gas to create plasma, which can cut through materials. Plasma beam arcs can reach extremely high temperatures, typically around 25,000 °C, making them among the hottest sources used in industrial cutting applications. Steel and sometimes other metals of different thicknesses are cut using the plasma cutting technique. Leading companies include Riland Industry Group, Ltd in China, Panasonic in Japan, and TAYOR in China. **Fig.12.** depicts a schematic diagram of a Plasma Beam cutting technique.

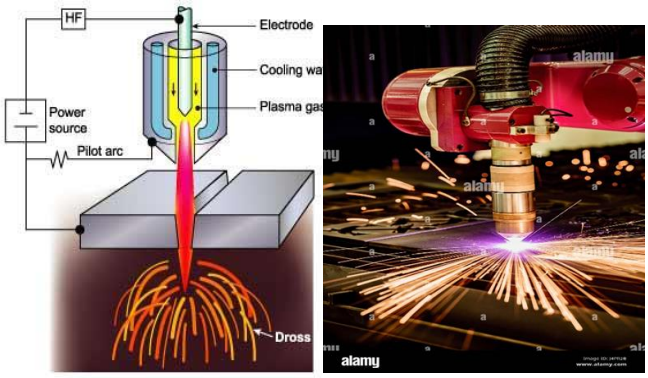

Fig. 12. Plasma beam cutting technique *(electricalfun.com and alamy.com)*

However, despite the progress made in existing research, studies in the field of laser, rust removal, surfacing, and cutting have primarily focused on the impact of a single factor, and few studies have considered the relationships between multiple factors and their overall impact on the quality of metal surface cleaning. This study aims to critique the viability of laser surfacing, rust removal, and cutting machine processes in industry. The following objectives are explored through a thorough literature review:

- Introduce the operations of laser surfacing, rust removal, and cutting
- Identify the advantages and disadvantages of these methods and compare them to other state-of-the-art techniques
- Identify the roles of different laser parameters on laser machining operations and determine how changing them affects the final product

The methodology adopted in this study is reported in Section 3; the main results obtained are discussed in Section 4; while the conclusions and recommendations are summarized in Section 5.

3. Methodology

3.1 Laser Surface Finishing Parameters

Though the physics behind laser remelting can be modelled numerically to a promising degree of accuracy, the parameters that control the laser's interaction with the material surface are critically important to the dynamics of the process and the quality of the result. Research conducted by Y. Cheng [8] reported that vital parameters for final material surfacing on the Ti6Al4V samples were laser power, laser scanning speed, and beam overlap, with the addition of ultrasonic vibration to prevent over-melting.

3.1.1 Laser Surface Finishing Experimental Setup

The experiment first establishes a numerical simulation of ultrasonic vibration-assisted laser polishing. A two-dimensional model in COMSOL Multiphysics was developed to simulate the melt pool. Assumptions of incompressible laminar flow, isotropic Ti6Al4V material properties, a Gaussian energy source confined to the surface, negligible frictional heating, and negligible material evaporation were made. The governing equations of transient heat transfer, latent heat via a specific heat formulation, and fluid mass and momentum conservation were applied along with volumetric forces for buoyancy, gravity, and ultrasonic vibration. This was modelled in a fine triangular mesh of 5 mm by 3 mm with cell sizes ranging from 0.001 to 0.035mm. The direct solver was then run to predict and model melt pool dynamics related to experimentally measured results (**Fig. 8,** *Laser surface finishing schematic experimental setup).*

The experimental laser system comprises an IPG YLR-500 laser, a laser polishing head, and a KUKA arm (model KR16-2). The laser system controls the laser to polish in the Y-direction. In contrast, the system applies ultrasonic vibration to the workpiece in the Z-direction, generating minute vertical oscillations. To systematically investigate the effect of ultrasonic vibration on the polishing, this study regulates the vibration amplitude by precisely controlling the ultrasonic power (UP). Specifically, when the UP was set to 5%, 10%, 15%, 20%, and 25%, the corresponding amplitudes were adjusted to 2.0 μ m, 2.7 μ m, 3.5 μ m, 4.2 μ m, and 5.0 μ m, respectively [38-39], [33], and [40]. The experimental specimens of Ti6Al4V were derived from the same batch to ensure uniform surface morphology. All specimens were uniformly brushed and cleaned with ethanol to remove any surface contaminants. The experimental Rz value and the simulation were found to be 1.745 μm and 1.586 μm, respectively. But a 9.1 % error. In UVLP, the experimental Rz value and the simulated Rz value were found to be 1.186 μm and 1.025 μm. Hence, an error of 13.6 %. These errors are within the acceptable range, confirming the accuracy of the simulation model [33].

3.1.2 Laser Power

Studies affirmed that low laser power, around 200 W, was insufficient to melt surface asperities due to suboptimal energy density. As the power increases to the range of 250–300 W, melting becomes more complete, and Marangoni and capillary flow dynamics begin to dominate, redistributing the material. Roughness fell to a minimum around 300W, but beyond this optimum, over-melting begins to occur, inducing oscillatory flows and creating waviness. The effects of laser cutting parameters on oxygen content, material removal rate, as proposed by D'aurelio et al. [38], are illustrated in **Fig. 13.**

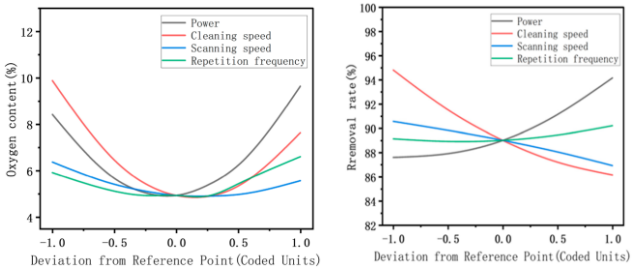

Fig. 13. Impact of interaction on various factors on oxygen & removal rate contents [38]

3.1.3 Laser Scanning Speed

Scanning speed at lower laser powers has virtually no impact, as it shortens interaction times between the material surface and the localized energy deposition from the laser. With a sufficient power level (> 250 W), experimental results indicate a positive correlation between scanning speed and surface roughness. As scanning speed increases, roughness is reduced by limiting excessive heat deposition, which promotes a thinner, better-controlled melt pool. Optimal conditions for reducing scanning speed surface roughness were determined experimentally at various laser power intensities (**Fig. 14).** These conditions were established at a laser power of 300 W and a scanning speed of 25 mm/s [33].

3.1.4 Laser Beam Overlap

Beam overlap dictates how successfully the laser surface is uniformly treated by the material surface. Moderate overlaps (25%-75% of beam diameter) produced consistent remelting of previously treated and solidified tracks. This was observed to have an inverse relationship with surface roughness, where roughness is reduced as the overlap increases. However, too high an overlap (> 75 %) leads to excessive heat accumulation, extending the duration of the surface being in a molten state, fostering thermal stresses, and coarser resolidified grain structures. This, in turn, reduces material surface hardness. Across all overlap rates tested, the combination of 300 W power, 25 mm/s scan speed, and a moderate overlap yielded the lowest roughness.

3.2 Laser Resurfacing (Cleaning) Parameters

Like all laser machining processes, the quality of a laser-cleaned surface depends heavily on the input parameters set for laser cleaning. For dry laser cleaning, the main forces that must be overcome to remove particles from the surface are van der Waals and electrostatic forces [6], [41 - 42]. For particles smaller than a few microns, van der Waals forces are dominant and can be represented by the equation:

$$F_v = \frac{hr}{8\pi z^2} + \frac{hr_c^2}{8\pi z^3} \tag{1}$$

Where r, h, and z are the radius of particles, the Van Der Waals constant, and the atomic spacing between the particles and the surface. The subsequent goal is to create a cleaning force greater than the Van Der Waals force, which will result in the ejection of particles. For larger contaminant particles, more energy is required to overcome the combination of electrostatic and van der Waals forces. The most important parameters for cleaning efficiency were identified as laser power, wavelength, pulse width, and scanning speed. They described an empirical formula for cleaning efficiency as:

$$C_E = cX \times \left(\frac{P}{A}\right)^n \times \left(\frac{t''t}{\tau_p t'}\right)^{n+1} \times \frac{1\,(\mathrm{m}^2)}{A\,(\mathrm{m}^2)} \tag{2}$$

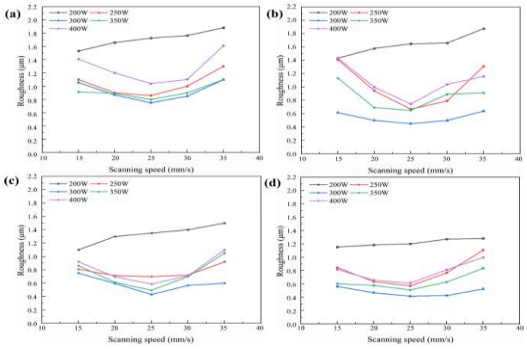

Fig. 14. Laser power and scanning speed effect on surface roughness at various beam overlap rates/amplitude of (a) 2.0%, (b) 50%, (c) 75%, (d) 85 % [33]

Where c and n represent the empirical constants depending on the target conditions and laser parameters, X represents the thickness of the contaminant, P is the average power, A is the area irradiated by the laser beam on the target surface, τ_p is the

pulse width, and t is the pulse duration. The result also shows that laser wavelength affects the absorption and reflectivity coefficients of the surface and affects the rise in temperature of particles lying on this surface. This is relevant in the following equation for the cleaning force of the laser:

$$F = \gamma E \Delta T(d, t) \quad (3)$$

Where: γ, E, ΔT, and (d, t) are the linear thermal expansion coefficient, elastic modulus, and temperature rise at the surface housing the particle, respectively [6].

3.3 Cutting Techniques Parameters

The industrial cutting methodology adopted in this study involves a comparative analysis of three metal-cutting techniques (water jet cutting, laser cutting, and plasma cutting). Hence, each is described in terms of its operational principles, advantages, and limitations. This structured approach ensures a comprehensive comparison of the cutting techniques, providing valuable insights for selecting the most suitable method for specific applications.

3.3.1 Concept of Data Collection

In this research, data are gathered from existing literature and experimental observations to evaluate the performance of each cutting method [15]. The techniques are compared based on these six key parameters:

- Versatility of technique cuts (economy cuts).
- Environmental impact
- Material thickness limitations
- Thermal deformation
- Cut surface quality
- Ease of programming

3.3.2 Cutting Experimental Setup

Works of literature affirmed that for water jet cutting, high-pressure water mixed with abrasive particles is used to cut materials. However, laser cutting employs a focused laser beam and technical gas to achieve precision cuts. Plasma cutting utilizes a high-temperature plasma arc to melt and remove material [19], [37], and [43 - 40]. In the comparative analysis of these three metal-cutting techniques, the effects of each method on the workpiece, including thermal deformation, surface quality, and material hardening, were also examined. The summary of the performance of the three methods across the evaluation criteria was presented in a tabular form in the section of this study. Hence, the strengths and weaknesses of each technique were also featured in the results.

4. Results and Discussion

4.1 Laser Surface Finishing Parameter Optimization

When conducting laser surface finishing on a material, it is important to understand the material properties of the parts being worked on to develop an optimal solution for laser treatment. Laser parameters, such as laser power, scanning speed, and beam overlap, are most prevalent. The final geometry of the part has an impact on the process. Hence, the criticality of having a properly programmed robotic or CNC control apparatus to ensure that the entire material surface can be treated.

4.2 Laser Resurfacing (Cleaning) Parameter Optimization

Similarly, for laser cleaning, the parameters of laser power, scanning speed, and pulse width impact the quality of the process and final surface finish. Optimizing the laser power and scanning speed to fully ablate corrosion, thereby keeping the underlying material surface intact. Due to the nature of laser ablation, laser pulses are used for high-energy deposition over short periods. As stated above, it is critical to find a pulse width that is narrow enough to deposit a high energy density to ablate the corrosion, but wide enough not to leave craters in the cleaned material surface. Due to the substantial costs often associated with trial-and-error approaches in these manufacturing techniques, it is highly beneficial to develop comprehensive numerical models that simulate the dynamics of laser-surface interactions and can be validated against experimental results, streamlining the parameter optimization process. The theoretical and empirical formulas above can also be used to estimate proper laser parameters.

Equation 1 suggests that increasing the laser intensity, either by increasing laser power or decreasing the focus area of the laser, will increase the cleaning efficiency. Similarly, Equation 2 suggests that the lower the wavelength of the laser, the greater the cleaning efficiency due to greater energy absorption by the surface and particles. The pulse width is a quite important parameter for determining how well the surface is cleaned in pulse laser cleaning. Zhu et al. [6] show, as expected, that an increase in pulse width results in greater energy absorption by the surface and particles. An increase in this energy absorption results in larger particles being able to be removed, but also increases the likelihood of damaging the surface. Narayanan et al. affirmed that slower scanning speeds result in deeper craters in the surface material [29]. This increases the amount of material to be removed at the cost of more damage to the surface. Much like pulse width, a slower scan speed allows the surface and particles to absorb more energy. It was observed that for a given laser power, there exists a laser scanning speed range that results in a change to

the crater depth created by the laser, suggesting an optimal scanning speed range for different laser powers and materials.

4.3 Cutting Techniques Parameter Optimization

Conclusions on these cutting techniques are drawn from experimental results in various kinds of literature. A comprehensive comparative analysis of waterjet, plasma, and laser industrial cutting techniques, incorporating key parameters such as versatility, environmental impact, material thickness limitations, thermal deformation, cut surface quality, ease of programming, cutting speed, workpiece geometry, operational costs, cutting precision and other critical factors is thoroughly presented in **Table 1**, based on the framework proposed by Krajcar et al. [37].

4.3.1 Key Parameter Result

Table 1: A comparative analysis report of water jet, laser, and plasma cutting techniques

Method of cutting	Abrasive Water Jet	Plasma beam	Laser beam
Speed	Slow	Fast	fast
Operating costs	Topmost	Lower	Lower
Precision cutting	High	Impossible	Higher
Size details	Small and large	Large	Small and large
Shapes	Complicated	Simple	Complicated
Thermal deformation	Lack	Yes, wider area	Yes, a small area
Material suitable for intersection	Most of the solid	Metals and conductive materials	Homogeneous with no reflective bodies
Materials covered with rust	Very good	Average	Good
Composite	Yes	No	No
Material hardening	No	Yes	Yes
Hazardous vapors	No	Yes	Yes
Multilayer cutting	Possible	Impossible	Impossible
Burr formation	Minimal	Yes	Yes
Material thickness	Thick and thin	Medium and thick	Thin and medium

The methodology section of this study emphasizes six critical cutting parameters identified through a comprehensive review of existing literature and experimental observations. These parameters were employed to assess the performance of waterjet, laser, and plasma cutting techniques. A concise summary of each parameter, as derived from the detailed literature review, is presented below.

- **Versatility:** Research affirmed that waterjet cutting excels in versatility, handling various materials, including reflective and non-conductive ones, unlike laser and plasma methods.
- **Environmental Impact:** Highlighted water-jet cutting is the most eco-friendly, using recyclable abrasives and water, while laser and plasma emit hazardous fumes.
- **Material Thickness Limitations:** Waterjet cutting handles thick materials over 100 mm, plasma cuts up to 160 mm, while laser struggles beyond 30 mm thickness.
- **Thermal Deformation:** Waterjet cutting avoids thermal deformation, preserving material integrity, whereas laser and plasma cause heat-induced structural changes.
- **Cut Surface Quality:** Waterjet cutting produces smooth, burr-free edges, plasma is rough and inaccurate, and laser cutting offers precision but heat-affected zones.
- **Ease of Programming:** All three methods allow easy programming, but water jetting requires minimal setup, ensuring stable material placement.

5. Conclusion

In conclusion, laser surfacing, resurfacing, and cutting are valuable laser machining operations that provide advantages not previously known to the machining industry. These state-of-the-art techniques aid in the sheet metal fabrication industry, additive manufacturing, and steel rehabilitation and cleaning, among others. While still considered the leading edge of technology, research trends show these methods are destined to become a staple in the machining industry for decades to come. The main results obtained from this study are:

- Laser surfacing improves surface finish on simple and complex geometries for a variety of materials through remelting and solidification of the work surface. Similarly, thermal expansion as well as pressure waves can remove unwanted particles such as rust and dirt in the case of laser cleaning (resurfacing). Laser cutting uses a High-Powered laser to create a melt pool that eventually cuts through material in a precise manner.
- These methods can efficiently and precisely perform across a wide range of complex geometries with little waste and no tool wear. Though difficult parameter selection and relatively high cost impose a barrier to using such technologies.

- The laser parameters of laser power and scanning speed are the most important parameters for determining the success of a laser machining operation; hence, they must be carefully selected based on the material and condition of the workpiece.

Authors recommend more findings in the areas of laser parameter selection and optimization, process implementation, and integration into existing manufacturing processes. While these methods show promise, many of the results seen in current research are on small scales in controlled environments. An utmost priority is required to achieve a better understanding of how to accurately set laser parameters, to process specific materials and workpieces without a trial-and-error method. The development of numerical methods and simulations has been explored, but general use cases have yet to be developed. In the additive manufacturing area, there is an opportunity to implement a laser polishing workflow, which would make the process much more desirable and cost-effective. Lastly, laser cleaning requires relatively large machines that might prohibit this method from being used in some cases. Hence, continuous studies to develop more mobile handheld technologies should be encouraged.

References

[1] Vinod, B. R., & Swetha, G. A. (2024). A Review of the Effects of Laser Cleaning on the Development of Corrosion and the Removal of Rust in Steel Bridges in Marine Environments. In *Laser-Assisted Machining: Processes and Applications* (pp. 87–113). wiley. https://doi.org/10.1002/9781394214655.ch7

[2] Jing, Z., Xu, Z., Min, Z., Haoyu, Z., Shengrong, Z. (2024). Research on the Technology of Laser Derusting and Design of Portable Laser Derusting System. In: Hung, J.C., Yen, N., Chang, JW. (eds) Frontier Computing on Industrial Applications Volume 3. FC 2023. Lecture Notes in Electrical Engineering, vol 1133. Springer, Singapore. https://doi.org/10.1007/978-981-99-9416-8_15

[3] Liu, Y., Li, C., Feng, L., & Han, X. (2024). Sensitivity analysis of the process parameters of the composite process of submerged arc surfacing and laser cladding. *International Journal of Advanced Manufacturing Technology*, *133*(9–10), 4777–4806. https://doi.org/10.1007/s00170-024-13842-y

[4] B. Guan, L. Qin, G. Yang, Y. Ren, X. Wang (2024). Laser Polishing of Directed Energy Deposition Metal Parts: A Review. *Additive Manufacturing Frontiers, Volume 3, Issue 4, 200174, ISSN 2950-4317* https://doi.org/10.1016/j.amf.2024.200174

[5] E.V. Bordachev, A.M.K. Hafiz, O.R. Tutunea-Fatan, Performance of laser polishing in finishing of metallic surfaces. *Int J Adv Manuf Technol* 73, 35–52, 2014, https://doi.org/10.1007/s00170-014-5761-3

[6] Zhu, G., Xu, Z., Jin, Y., Chen, X., Yang, L., Xu, J., Shan, D., Chen, Y., & Guo, B. (2022). Mechanism and application of laser cleaning: A review. In *Optics and Lasers in Engineering* (Vol. 157). Elsevier Ltd. https://doi.org/10.1016/j.optlaseng.2022.107130

[7] Chen, Y., Deng, G., Zhou, Q., & Feng, G. (2020). Acoustic signal monitoring in laser paint cleaning. *Laser Physics*, *30*(6), 066001–066001. https://doi.org/10.1088/1555-6611/ab85c7

[8] Y. Cheng, P. Zou, L. Kong, B. Li, Y. Zhang (2025) Research on the effect of ultrasonic vibration-assisted laser polishing (UVLP) on Ti6Al4V surface properties and establishment of roughness prediction model, *Optics & Laser Technology, Volume 186, 2025, 112714, ISSN 0030-3992,* https://doi.org/10.1016/j.optlastec.2025.112714

[9] Lu, Y.-F., Zhang, Y., Song, W.-D., & Daniel. (1998). A Theoretical Model for Laser Cleaning of Microparticles in a Thin Liquid Layer. *Japanese Journal of Applied Physics*, *37*(11A), L1330–L1330. https://doi.org/10.1143/jjap.37.l1330

[10] Frank, P., Lang, F., Mosbacher, M., J. Boneberg, & P. Leiderer. (2008). Infrared steam laser cleaning. *Applied Physics A*, *93*(1), 1–4. https://doi.org/10.1007/s00339-008-4651-7

[11] Jang, D., Lee, J., Lee, J.-M., & Kim, D. (2008). Visualization of particle trajectories in the laser shock cleaning process. *Applied Physics A*, *93*(1), 147–151. https://doi.org/10.1007/s00339-008-4659-z

[12] Alsaadawy, M., Dewidar, M., Said, A., Maher, I., & Shehab Eldeen, T. A. (2024). A comprehensive review of the influence of laser cutting parameters on surface and kerf quality of metals. In *International Journal of Advanced Manufacturing Technology* (Vol. 130, Issues 3–4, pp. 1039–1074). Springer Science and Business Media Deutschland GmbH. https://doi.org/10.1007/s00170-023-12768-1

[13] Rajaram, N., Sheikh-Ahmad, J., & S. Hossein Cheraghi. (2003). *CO2 laser cut quality of 4130 steel*. *43*(4), 351–358. https://doi.org/10.1016/s0890-6955(02)00270-5

[14] Senthilkumar, V. (2014). *Laser Cutting Process – A Review*. ResearchGate. https://www.researchgate.net/publication/305385939_Laser_cutting_process_-_A_Review

[15] Irsel, G., & Güzey, B. N. (2021). Comparison of laser beam, oxygen, and plasma arc cutting methods in terms of their advantages and disadvantages in cutting structural steels. *Journal of Physics: Conference Series*, *2130*(1). https://doi.org/10.1088/1742-6596/2130/1/012022

[16] Dolgova, S., Malikov, A., Golyshev, A., & Nikulina, A. (2024). The effect of laser surfacing modes on the geometrical characteristics of the single laser tracks. *Obrabotka Metallov*, *26*(2), 57–70. https://doi.org/10.17212/1994-6309-2024-26.2-57-70

[17] Biryukov, V. (2024). Increasing the wear resistance of agricultural machinery parts by laser surfacing. *E3S Web of Conferences*, *592*. https://doi.org/10.1051/e3sconf/202459205020

[18] Caggiano, A., Teti, R., Alfieri, V., & Caiazzo, F. (2021). Automated laser polishing for surface finish

enhancement of additive-manufactured components for the automotive industry. *Production Engineering*, *15*(1), 109–117. https://doi.org/10.1007/s11740-020-01007-1

[19] W. Wang, P. Zou, J. Xu, K. F. Ehmann (2023) Surface morphology evolution mechanisms of laser polishing in ambient gas, *International Journal of Mechanical Sciences, Volume 250, 2023, 108302, ISSN 0020-7403,* https://doi.org/10.1016/j.ijmecsci.2023.108302

[20] Basha, S. M., Bhuyan, M., Basha, M. M., Venkaiah, N., & Sankar, M. R. (2019). Laser polishing of 3D printed metallic components: A review on surface integrity. *Materials Today: Proceedings*, *26*, 2047–2054. https://doi.org/10.1016/j.matpr.2020.02.443

[21] Abhishek Kumar, Harikrishnan Ramadas, Cheruvu Siva Kumar, Ashish Kumar Nath, Laser polishing of additive manufactured stainless-steel parts by line focused beam: A response surface method for improving surface finish, *Journal of Manufacturing Processes*, Volume 133, 2025, Pages 1310-1328, ISSN 1526-6125, https://doi.org/10.1016/j.jmapro.2024.12.028

[22] Ermergen, T., & Taylan, F. (2021). Review on Surface Quality Improvement of Additively Manufactured Metals by Laser Polishing. In *Arabian Journal for Science and Engineering* (Vol. 46, Issue 8, pp. 7125–7141). Springer Science and Business Media Deutschland GmbH. https://doi.org/10.1007/s13369-021-05658-9

[23] Haoxiang Lu, Dazhong Wang, Shujing Wu, Zili Pan, Guoqiang Wang, Guoqiang Guo, Yebing Tian, Daohui Xiang, A Review Of Laser Polishing on Ti6Al4V Based On Energy Density, *Journal of Materials Processing Technology,* Volume 331, 2024, 118520, ISSN 0924-0136, https://doi.org/10.1016/j.jmatprotec.2024.118520

[24] Jinan, L., Yanhe, S., Yuan, F., Jun, T., Chunyu, F., Hua, Z., & Chengbing, Z. (2020). Mechanism Research and Equipment Development of Laser Cleaning Rust. *Journal of Physics: Conference Series*, *1453*(1). https://doi.org/10.1088/1742-6596/1453/1/012041

[25] Narayanan, V., Singh, R., & Marla, D. (2025). Optimization of Nanosecond Pulsed Laser Cleaning of Rust. *Lasers in Manufacturing and Materials Processing*. https://doi.org/10.1007/s40516-025-00282-z

[26] Gisario, A., Barletta, M. & Veniali, F. Laser polishing: a review of a constantly growing technology in the surface finishing of components made by additive manufacturing. *Int J Adv Manuf Technol* 120, 1433–1472 (2022). https://doi.org/10.1007/s00170-022-08840-x

[27] Guan, B., Qin, L., Yang, G., Ren, Y., & Wang, X. (2024). Laser polishing of directed energy deposition metal parts: A review. In *Additive Manufacturing Frontiers* (Vol. 3, Issue 4). Elsevier B.V. https://doi.org/10.1016/j.amf.2024.200174

[28] Zheng, Z., Wang, C., Huang, G., Feng, W., & Liu, D. (2021). Effect of defocused nanosecond laser paint removal on mild steel substrate in the ambient atmosphere. *Materials*, *14*(20). https://doi.org/10.3390/ma14205969

[29] Narayanan, V., Singh, R. K., & Marla, D. (2018). Laser cleaning for rust removal on mild steel: An experimental study on surface characteristics. *MATEC Web of Conferences*, *221*. https://doi.org/10.1051/matecconf/201822101007

[30] He, Y., Cai, X., & Ye, J. (2023). Research on pulse laser cleaning and rust removal technology in power systems. *AIP Advances*, *13*(9). https://doi.org/10.1063/5.0155263

[31] Garcia-Fernandez, J., Salguero, J., Batista, M., Vazquez-Martinez, J. M., & del Sol, I. (2024). Laser Surface Texturing of Cutting Tools for Improving the Machining of Ti6Al4V: A Review. In *Metals* (Vol. 14, Issue 12). Multidisciplinary Digital Publishing Institute (MDPI). https://doi.org/10.3390/met14121422

[32] Klich, L., Marciniak, M., & Sikorska-Czupryna, S. (2025). Optimization of the laser cutting process by integrating an automatic storage and loading system with enterprise resource management integration. *Advances in Science and Technology Research Journal*, *19*(4), 365–376. https://doi.org/10.12913/22998624/200725

[33] Ni, C., Zhu, J., Zhang, B., An, K., Wang, Y., Liu, D., Lu, W., Zhu, L., & Liu, C. (2025). Recent advances in laser powder bed fusion of Ti–6Al–4V alloys: microstructure, mechanical properties, and machinability. In *Virtual and Physical Prototyping* (Vol. 20, Issue 1). Taylor and Francis Ltd. https://doi.org/10.1080/17452759.2024.2446952

[34] Wang, G., Deng, J., Lei, J., Tang, W., Zhou, W., & Lei, Z. (2024). Multi-Objective Optimization of Laser Cleaning Quality of Q390 Steel Rust Layer Based on Response Surface Methodology and NSGA-II Algorithm. *Materials*, *17*(13). https://doi.org/10.3390/ma17133109

[35] Ngadiono, Y., Saputra, D. A., Setiadi, B. R., & Pardjono, P. (2025). Taguchi's Method for Optimum Cutting of Acrylic Materials on a 40-Watt CNC Laser Cutting Machine. *TEM Journal*, 933–939. https://doi.org/10.18421/TEM141-82

[36] Naresh, & Khatak, P. (2022). Laser cutting technique: A literature review. *Materials for Today: Proceedings*, *56*, 2484–2489. https://doi.org/10.1016/j.matpr.2021.08.250

[37] Krajcar, D. (2014). Comparison of metal water jet cutting with laser and plasma cutting. *Procedia Engineering*, *69*, 838–843. https://doi.org/10.1016/j.proeng.2014.03.061

[38] D'aurelio, G., Chita, G., & Cinquepalmi, M. (n.d.). Laser surface cleaning, de-rusting, de-painting, and de-oxidizing. *Appl. Phys. A*, *69*. https://doi.org/10.1007/s003399900373

[39] Di Kang, Ping Zou, Hao Wu, Wenjie Wang, Jilin Xu, Research on ultrasonic vibration-assisted laser polishing of the 304 stainless steel, *Journal of Manufacturing Processes*, Volume 62, 2021, Pages 403-417, ISSN 1526-6125, https://doi.org/10.1016/j.jmapro.2020.12.009

[40] Manco, E., Cozzolino, E., & Astarita, A. (2022). Laser polishing of additively manufactured metal parts: a review. In *Surface Engineering* (Vol. 38, Issue 3, pp. 217–233). Taylor and Francis Ltd. https://doi.org/10.1080/02670844.2022.2072080

[41] Belosludtsev, A., Bitinaitis, I., Baltrušaitis, K., & Rodin, A. M. (n.d.). *Investigation of the laser cleaning process*

for IBS grids in optical coating technology. https://doi.org/10.1007/s00170-021-07035-0/Published

[42] Zhang, H., Zhang, J., Zhang, X., Zhu, S., & Zhang, M. (2023). Analysis of Laser Cleaning and Rust Removal Technology for Substation Isolator Switches. *Journal of Physics: Conference Series*, *2488*(1). https://doi.org/10.1088/1742-6596/2488/1/012033

[43] Wang, W. (2023). Surface defects detection in metal materials repaired by laser surfacing of seal welds. *Journal of Measurements in Engineering*, *11*(3), 343–357. https://doi.org/10.21595/jme.2023.23316

[44] Yue, L., Wang, Z., & Li, L. (2012). Multiphysics modelling and simulation of dry laser cleaning of micro-slots with particle contaminants. *Journal of Physics D Applied Physics*, *45*(13), 135401–135401. https://doi.org/10.1088/0022-3727/45/13/135401

INTERNATIONAL JOURNAL OF ENGINEERING TECHNOLOGIES-IJET

Guide for Authors

The **International Journal of Engineering Technologies (IJET)** seeks to promote and disseminate knowledge of the various topics of engineering technologies. The journal aims to present to the international community important results of work in the fields of engineering such as imagining, researching, planning, creating, testing, improving, implementing, using and asking. The journal also aims to help researchers, scientists, manufacturers, institutions, world agencies, societies, etc. to keep up with new developments in theory and applications and to provide alternative engineering solutions to current.

The *International Journal of Engineering Technologies* is a quarterly published journal and operates an online submission and peer review system allowing authors to submit articles online and track their progress via its web interface. The journal aims for a publication speed of **60 days** from submission until final publication.

The coverage of IJET includes the following engineering areas, but not limited to:

All filed of engineering such as;

Chemical engineering

- Biomolecular engineering
- Materials engineering
- Molecular engineering
- Process engineering

Civil engineering

- Environmental engineering
- Geotechnical engineering
- Structural engineering
- Transport engineering
- Water resources engineering

Electrical engineering

- Computer engineering
- Electronic engineering
- Optical engineering
- Power engineering

Mechanical engineering

- Acoustical engineering
- Manufacturing engineering
- Thermal engineering
- Vehicle engineering

Systems (interdisciplinary) engineering

- Aerospace engineering
- Agricultural engineering
- Applied engineering
- Biological engineering
- Building services engineering
- Energy engineering
- Railway engineering
- Industrial engineering
- Mechatronics
- Military engineering
- Nano engineering
- Nuclear engineering
- Petroleum engineering

Types of Articles submitted should be original research papers, not previously published, in one of the following categories,

- Applicational and design studies.
- Technology development,

– Comparative case studies.

– Reviews of special topics.

– Reviews of work in progress and facilities development.

– Survey articles.

– Guest editorials for special issues.

Ethic Responsibilities

The publication of an article in peer-reviewed *"International Journal of Engineering Technologies"* is an essential building block in the development of a coherent and respected network of knowledge. It is a direct reflection of the quality of the work. Peer-reviewed articles support and embody the scientific method. It is therefore important to agree upon standards of expected ethical behavior for all parties involved in the act of publishing: the author, the journal editor, the peer reviewer, the publisher and the society of society-owned or sponsored journals.

All authors are requested to disclose any actual or potential conflict of interest including any financial, personal or other relationships with other people or organizations within three years of beginning the submitted work that could inappropriately influence, or be perceived to influence, their work.

Submission of an article implies that the work described has not been published previously that it is not under consideration for publication elsewhere. The submission should be approved by all authors and tacitly or explicitly by the responsible authorities where the work was carried out, and that, if accepted, it will not be published elsewhere in the same form, in English or in any other language, including electronically without the written consent of the copyright-holder.

Upon acceptance of an article, authors will be asked to complete a "Copyright Form". Acceptance of the agreement will ensure the widest possible dissemination of information. An e-mail will be sent to the corresponding author confirming receipt of the manuscript together with a "Copyright Form" form or a link to the online version of this agreement.

Author Rights

As a journal author, you retain rights for a large number of author uses, including use by your employing institute or company. These rights are retained and permitted without the need to obtain specific permission from *IJET.* These include:

- The right to make copies (print or electronic) of the journal article for your own personal use, including for your own classroom teaching use;
- The right to make copies and distribute copies (including via e-mail) of the journal article to research colleagues, for personal use by such colleagues for scholarly purposes;
- The right to post a pre-print version of the journal article on internet web sites including electronic pre-print servers, and to retain indefinitely such version on such servers or sites for scholarly purposes
- the right to post a revised personal version of the text of the final journal article on your personal or institutional web site or server for scholarly purposes
- The right to use the journal article or any part thereof in a printed compilation of your works, such as collected writings or lecture notes.

Article Style

Authors must strictly follow the guide for authors, or their articles may be rejected without review. Editors reserve the right to adjust the style to certain standards of uniformity. Follow Title, Authors, Affiliations, Abstract, Keywords, Introduction, Materials and Methods, Theory/Calculation, Conclusions, Acknowledgements, References order when typing articles. The corresponding author should be identified with an asterisk and footnote. Collate

acknowledgements in a separate section at the end of the article and do not include them on the title page, as a footnote to the title or otherwise.

Abstract and Keywords:

Enter an abstract of up to 250 words for all articles. This is a concise summary of the whole paper, not just the conclusions, and is understandable without reference to the rest of the paper. It should contain no citation to other published work. Include up to six keywords that describe your paper for indexing purposes.

Abbreviations and Acronyms:

Define abbreviations and acronyms the first time they are used in the text, even if they have been defined in the abstract. Abbreviations such as IEEE, SI, MKS, CGS, sc, dc, and rms do not have to be defined. Do not use abbreviations in the title unless they are unavoidable.

Text Layout for Peer Review:

Use single column layout, double spacing and wide (3 cm) margins on white paper at the peer review stage. Ensure that each new paragraph is clearly indicated. Present tables and figure legends in the text where they are related and cited. Number all pages consecutively; use 12 pt font size and standard fonts; Times New Roman, Helvetica, or Courier is preferred.

Research Papers should not exceed 12 printed pages in two-column publishing format, including figures and tables.

Technical Notes and *Letters* should not exceed 2,000 words.

Reviews should not exceed 20 printed pages in two-column publishing format, including figures and tables.

Equations:

Number equations consecutively with equation numbers in parentheses flush with the right margin, as in (1). To make equations more compact, you may use the solidus (/), the exp function, or appropriate exponents. Italicize Roman symbols for quantities and variables, but not Greek symbols. Use an dash (–) rather than a hyphen for a minus sign. Use parentheses to avoid ambiguities in denominators. Punctuate equations with commas or periods when they are part of a sentence, as in

$$C = a + b \qquad (1)$$

Symbols in your equation should be defined before the equation appears or immediately following. Use “Eq. (1)” or “equation (1),” while citing.

Figures and Tables:

All illustrations must be supplied at the correct resolution:

* Black and white and colour photos - 300 dpi

* Graphs, drawings, etc - 800 dpi preferred; 600 dpi minimum

* Combinations of photos and drawings (black and white and color) - 500 dpi

In addition to using figures in the text, upload each figure as a separate file in either .tiff or .eps format during submission, with the figure number.

Table captions should be written in the same format as figure captions; for example, “Table 1. Appearance styles.”. Tables should be referenced in the text unabbreviated as “Table 1.”

References:

Please ensure that every reference cited in the text is also present in the reference list (and viceversa). Any references cited in the abstract must be given in full. Unpublished results and personal communications are not recommended in the reference list, but may be mentioned in the text. Citation of a reference as “in press” implies that the item has been accepted for publication. Number citations consecutively in square brackets [1]. Punctuation follows the bracket [2]. Refer simply to the reference number, as in [3]. Use “Ref. [3]” or Reference [3]” at the beginning of a sentence: “Reference [3] was …”. Give all authors’ names; use “et al.” if there are six authors or more. For papers published in translated journals, first give the English citation, then the original foreign-language citation.

Books

[1] J. Clerk Maxwell*, A Treatise on Electricity and Magnetism,* 3rd ed., vol. 2. Oxford:Clarendon Press, 1892, pp.68-73.

Journals

[2] Y. Yorozu, M. Hirano, K. Oka, and Y. Tagawa, “Electron spectroscopy studies on magneto-optical media and plastic substrate interface”, *IEEE Transl. J. Magn. Japan*, vol. 2, pp. 740-741, August 1987.

Conferences

[3] Çolak I., Kabalci E., Bayindir R., and Sagiroglu S, “The design and analysis of a 5-level cascaded voltage source inverter with low THD”, *2nd PowerEng Conference*, Lisbon, pp. 575-580, 18-20 March 2009.

Reports

[4] IEEE Standard 519-1992, Recommended practices and requirements for harmonic control in electrical power systems, *The Institute of Electrical and Electronics Engineers*, 1993.

Text Layout for Accepted Papers:

A4 page margins should be margins: top = 24 mm, bottom = 24 mm, side = 15 mm. Main text should be given in two column. The column width is 87mm (3.425 in). The space between the two columns is 6 mm (0.236 in). Paragraph indentation is 3.5 mm (0.137 in). Follow the type sizes specified in Table. Position figures and tables at the tops and bottoms of columns. Avoid placing them in the middle of columns. Large figures and tables may span across both columns. Figure captions should be centred below the figures; table captions should be centred above. Avoid placing figures and tables before their first mention in the text. Use the abbreviation “Fig. 1,” even at the beginning of a sentence.

Type size (pts.)	Appearance		
	Regular	**Bold**	*Italic*
10	Authors' affiliations, Section titles, references, tables, table names, first letters in table captions,figure captions, footnotes, text subscripts, and superscripts	**Abstract**	
12	Main text, equations, Authors' names, [a]		*Subheading (1.1.)*
24	Paper title		

Submission checklist:

It is hoped that this list will be useful during the final checking of an article prior to sending it to the journal's Editor for review. Please consult this Guide for Authors for further details of any item. Ensure that the following items are present:

- ❖ One Author designated as corresponding Author:

• E-mail address

• Full postal address

• Telephone and fax numbers

- ❖ All necessary files have been uploaded

• Keywords: a minimum of 4

• All figure captions (supplied in a separate document)

• All tables (including title, description, footnotes, supplied in a separate document)

- ❖ Further considerations

• Manuscript has been "spellchecked" and "grammar-checked"

• References are in the correct format for this journal

• All references mentioned in the Reference list are cited in the text, and vice versa

• Permission has been obtained for use of copyrighted material from other sources (including the Web)

• Color figures are clearly marked as being intended for color reproduction on the Web (free of charge) and in print or to be reproduced in color on the Web (free of charge) and in black-and-white in print.

Article Template Containing Author Guidelines for Peer-Review

First Author*, Second Author**‡, Third Author***

*Department of First Author, Faculty of First Author, Affiliation of First Author, Postal address

**Department of Second Author, Faculty of First Author, Affiliation of First Author, Postal address

***Department of Third Author, Faculty of First Author, Affiliation of First Author, Postal address

(First Author Mail Address, Second Author Mail Address, Third Author Mail Address)

‡ Corresponding Author; Second Author, Postal address, Tel: +90 312 123 4567, Fax: +90 312 123 4567,corresponding@affl.edu

Received: xx.xx.xxxx Accepted:xx.xx.xxxx

Abstract- Enter an abstract of up to 250 words for all articles. This is a concise summary of the whole paper, not just the conclusions, and is understandable without reference to the rest of the paper. It should contain no citation to other published work. Include up to six keywords that describe your paper for indexing purposes. Define abbreviations and acronyms the first time they are used in the text, even if they have been defined in the abstract. Abbreviations such as IEEE, SI, MKS, CGS, sc, dc, and rms do not have to be defined. Do not use abbreviations in the title unless they are unavoidable.

Keywords- Keyword1; keyword2; keyword3; keyword4; keyword5.

2. Introduction

Authors should any word processing software that is capable to make corrections on misspelled words and grammar structure according to American or Native English. Authors may get help by from word

processor by making appeared the paragraph marks and other hidden formatting symbols. This sample article is prepared to assist authors preparing their articles to IJET.

Indent level of paragraphs should be 0.63 cm (0.24 in) in the text of article. Use single column layout, double-spacing and wide (3 cm) margins on white paper at the peer review stage. Ensure that each new paragraph is clearly indicated. Present tables and figure legends in the text where they are related and cited. Number all pages consecutively; use 12 pt font size and standard fonts; Times New Roman, Helvetica, or Courier is preferred. Indicate references by number(s) in square brackets in line with the text. The actual authors can be referred to, but the reference number(s) must always be given. Example: "..... as demonstrated [3, 6]. Barnaby and Jones [8] obtained a different result ...."

IJET accepts submissions in three styles that are defined as Research Papers, Technical Notes and Letter, and Review paper. The requirements of paper are as listed below:

- Research Papers should not exceed 12 printed pages in two-column publishing format, including figures and tables.
- Technical Notes and Letters should not exceed 2,000 words.
- Reviews should not exceed 20 printed pages in two-column publishing format, including figures and tables.

Authors are requested write equations using either any mathematical equation object inserted to word processor or using independent equation software. Symbols in your equation should be defined before the equation appears or immediately following. Use “Eq. (1)” or “equation (1),” while citing. Number equations consecutively with equation numbers in parentheses flush with the right margin, as in Eq. (1). To make equations more compact, you may use the solidus (/), the exp function, or appropriate exponents. Italicize Roman symbols for quantities and variables, but not Greek symbols. Use an dash (–) rather than a hyphen for a minus sign. Use parentheses to avoid ambiguities in denominators. Punctuate equations with commas or periods when they are part of a sentence, as in

$$C = a + b \tag{1}$$

Section titles should be written in bold style while sub section titles are italic.

3. Figures and Tables

3.1. Figure Properties

All illustrations must be supplied at the correct resolution:

- Black and white and colour photos - 300 dpi
- Graphs, drawings, etc - 800 dpi preferred; 600 dpi minimum
- Combinations of photos and drawings (black and white and colour) - 500 dpi

In addition to using figures in the text, Authors are requested to upload each figure as a separate file in either .tiff or .eps format during submission, with the figure number as Fig.1., Fig.2a and so on. Figures are cited as “Fig.1” in sentences or as “Figure 1” at the beginning of sentence and paragraphs. Explanations related to figures should be given before figure. Figures and tables should be located at the top or bottom side of paper as done in accepted article format.

Figure 1. Engineering technologies.

Table captions should be written in the same format as figure captions; for example, “Table 1. Appearance styles.”. Tables should be referenced in the text unabbreviated as “Table 1.”

Table 1. Appearance properties of accepted manuscripts

Type size (pts.)	Appearance		
	Regular	**Bold**	*Italic*
10	Authors’ affiliations, Abstract, keywords, references, tables, table names, figure captions, footnotes, text subscripts, and superscripts	**Abstract**	
12	Main text, equations, Authors’ names, Section titles		*Subheading (1.1.)*
24	Paper title		

4. Submission Process

The *International Journal of Engineering Technologies* operates an online submission and peer review system that allows authors to submit articles online and track their progress via a web interface. Articles that are prepared referring to this template should be controlled according to submission checklist given in “Guide f Authors”. Editor handles submitted articles to IJET primarily in order to control in terms of compatibility to aims and scope of Journal.

Articles passed this control are checked for grammatical and template structures. If article passes this control too, then reviewers are assigned to article and Editor gives a reference number to paper. Authors registered to online submission system can track all these phases.

Editor also informs authors about processes of submitted article by e-mail. Each author may also apply to Editor via online submission system to review papers related to their study areas. Peer review is a critical element of publication, and one of the major cornerstones of the scientific process. Peer Review serves two key functions:

- Acts as a filter: Ensures research is properly verified before being published
- Improves the quality of the research

5. Conclusion

The conclusion section should emphasize the main contribution of the article to literature. Authors may also explain why the work is important, what are the novelties or possible applications and extensions. Do not replicate the abstract or sentences given in main text as the conclusion.

Acknowledgements

Authors may acknowledge to any person, institution or department that supported to any part of study.

References

[1] J. Clerk Maxwell, *A Treatise on Electricity and Magnetism*, 3rd ed., vol. 2. Oxford:Clarendon Press, 1892, pp.68-73. (Book)

[2] H. Poor, *An Introduction to Signal Detection and Estimation*, New York: Springer-Verlag, 1985, ch. 4. (Book Chapter)

[3] Y. Yorozu, M. Hirano, K. Oka, and Y. Tagawa, "Electron spectroscopy studies on magneto-optical media and plastic substrate interface", *IEEE Transl. J. Magn. Japan*, vol. 2, pp. 740-741, August 1987. (Article)

[4] E. Kabalcı, E. Irmak, I. Çolak, "Design of an AC-DC-AC converter for wind turbines", *International Journal of Energy Research*, Wiley Interscience, DOI: 10.1002/er.1770, Vol. 36, No. 2, pp. 169-175. (Article)

[5] I. Çolak, E. Kabalci, R. Bayindir R., and S. Sagiroglu, "The design and analysis of a 5-level cascaded voltage source inverter with low THD", *2nd PowerEng Conference*, Lisbon, pp. 575-580, 18-20 March 2009. (Conference Paper)

[6] IEEE Standard 519-1992, Recommended practices and requirements for harmonic control in electrical power systems, *The Institute of Electrical and Electronics Engineers*, 1993. (Standards and Reports)

Article Template Containing Author Guidelines for Accepted Papers

First Author*, Second Author**‡, Third Author***

*Department of First Author, Faculty of First Author, Affiliation of First Author, Postal address

**Department of Second Author, Faculty of First Author, Affiliation of First Author, Postal address

***Department of Third Author, Faculty of First Author, Affiliation of First Author, Postal address

(First Author Mail Address, Second Author Mail Address, Third Author Mail Address)

‡ Corresponding Author; Second Author, Postal address, Tel: +90 312 123 4567,

Fax: +90 312 123 4567,corresponding@affl.edu

Received: xx.xx.xxxx Accepted:xx.xx.xxxx

Abstract- Enter an abstract of up to 250 words for all articles. This is a concise summary of the whole paper, not just the conclusions, and is understandable without reference to the rest of the paper. It should contain no citation to other published work. Include up to six keywords that describe your paper for indexing purposes. Define abbreviations and acronyms the first time they are used in the text, even if they have been defined in the abstract. Abbreviations such as IEEE, SI, MKS, CGS, sc, dc, and rms do not have to be defined. Do not use abbreviations in the title unless they are unavoidable.

Keywords Keyword1, keyword2, keyword3, keyword4, keyword5.

1. Introduction

Authors should any word processing software that is capable to make corrections on misspelled words and grammar structure according to American or Native English. Authors may get help by from word processor by making appeared the paragraph marks and other hidden formatting symbols. This sample article is prepared to assist authors preparing their articles to IJET.

Indent level of paragraphs should be 0.63 cm (0.24 in) in the text of article. Use single column layout, double-spacing and wide (3 cm) margins on white paper at the peer review stage. Ensure that each new paragraph is clearly indicated. Present tables and figure legends in the text where they are related and cited. Number all pages consecutively; use 12 pt font size and standard fonts; Times New Roman, Helvetica, or Courier is preferred. Indicate references by number(s) in square brackets in line with the text. The actual authors can be referred to, but the reference number(s) must always be given. Example: "..... as demonstrated [3,6]. Barnaby and Jones [8] obtained a different result ...."

IJET accepts submissions in three styles that are defined as Research Papers, Technical Notes and Letter, and Review paper. The requirements of paper are as listed below:

- Research Papers should not exceed 12 printed pages in two-column publishing format, including figures and tables.
- Technical Notes and Letters should not exceed 2,000 words.
- Reviews should not exceed 20 printed pages in two-column publishing format, including figures and tables.

Authors are requested write equations using either any mathematical equation object inserted to word processor or using independent equation software. Symbols in your equation should be defined before the equation appears or immediately following. Use “Eq. (1)” or “equation (1),” while citing. Number equations consecutively with equation numbers in parentheses flush with the right margin, as in Eq. (1). To make equations more compact, you may use the solidus (/), the exp function, or appropriate exponents. Italicize Roman symbols for quantities and variables, but not Greek symbols. Use an dash (-) rather than a hyphen for a

minus sign. Use parentheses to avoid ambiguities in denominators. Punctuate equations with commas or periods when they are part of a sentence, as in

$$C = a + b \quad (1)$$

Section titles should be written in bold style while sub section titles are italic.

6. Figures and Tables

6.1. Figure Properties

All illustrations must be supplied at the correct resolution:

- Black and white and colour photos - 300 dpi
- Graphs, drawings, etc - 800 dpi preferred; 600 dpi minimum
- Combinations of photos and drawings (black and white and colour) - 500 dpi

In addition to using figures in the text, Authors are requested to upload each figure as a separate file in either .tiff or .eps format during submission, with the figure number as Fig.1., Fig.2a and so on. Figures are cited as "Fig.1" in sentences or as "Figure 1" at the beginning of sentence and paragraphs. Explanations related to figures should be given before figure.

Fig. 1. Engineering technologies.

Figures and tables should be located at the top or bottom side of paper as done in accepted article format. Table captions should be written in the same format as figure captions; for example, "Table 1. Appearance styles.". Tables should be referenced in the text unabbreviated as "Table 1."

Table 1. Appearance properties of accepted manuscripts

Type size (pts.)	Appearance		
	Regular	**Bold**	*Italic*
10	Main text, section titles, authors' affiliations, abstract, keywords, references, tables, table names, figure captions, equations, footnotes, text subscripts, and superscripts	**Abstract-**	*Subheading (1.1.)*
12	Authors' names,		
24	Paper title		

6.2. Text Layout for Accepted Papers

A4 page margins should be margins: top = 24 mm, bottom = 24 mm, side = 15 mm. The column width is 87mm (3.425 in). The space between the two columns is 6 mm (0.236 in). Paragraph indentation is 3.5 mm (0.137 in). Follow the type sizes specified in Table. Position figures and tables at the tops and bottoms of columns. Avoid placing them in the middle of columns. Large figures and tables may span across both columns. Figure captions should be centred below the figures; table captions should be centred above. Avoid placing figures and tables before their first mention in the text. Use the abbreviation "Fig. 1," even at the beginning of a sentence.

7. Submission Process

The International Journal of Engineering Technologies operates an online submission and peer review system that allows authors to submit articles online and track their progress via a web interface. Articles that are prepared referring to this template should be controlled according to submission checklist given in "Guide f Authors". Editor handles submitted articles to IJET primarily in order to control in terms of compatibility to aims and scope of Journal. Articles passed this control are checked for grammatical and template structures. If article passes this control too, then reviewers are assigned to article and Editor gives a reference number to paper. Authors registered to online submission system can track all these phases. Editor also informs authors about processes of submitted article by e-mail. Each author may also apply to Editor via online

submission system to review papers related to their study areas. Peer review is a critical element of publication, and one of the major cornerstones of the scientific process. Peer Review serves two key functions:

- Acts as a filter: Ensures research is properly verified before being published
- Improves the quality of the research

8. Conclusion

The conclusion section should emphasize the main contribution of the article to literature. Authors may also explain why the work is important, what are the novelties or possible applications and extensions. Do not replicate the abstract or sentences given in main text as the conclusion.

Acknowledgements

Authors may acknowledge to any person, institution or department that supported to any part of study.

References

[7] J. Clerk Maxwell, A Treatise on Electricity and Magnetism, 3rd ed., vol. 2. Oxford:Clarendon Press, 1892, pp.68-73. (Book)

[8] H. Poor, An Introduction to Signal Detection and Estimation, New York: Springer-Verlag, 1985, ch. 4. (Book Chapter)

[9] Y. Yorozu, M. Hirano, K. Oka, and Y. Tagawa, "Electron spectroscopy studies on magneto-optical media and plastic substrate interface", IEEE Transl. J. Magn. Japan, vol. 2, pp. 740-741, August 1987. (Article)

[10] E. Kabalcı, E. Irmak, I. Çolak, "Design of an AC-DC-AC converter for wind turbines", International Journal of Energy Research, Wiley Interscience, DOI: 10.1002/er.1770, Vol. 36, No. 2, pp. 169-175. (Article)

[11] I. Çolak, E. Kabalci, R. Bayindir R., and S. Sagiroglu, "The design and analysis of a 5-level cascaded voltage source inverter with low THD", 2nd PowerEng Conference, Lisbon, pp. 575-580, 18-20 March 2009. (Conference Paper)

[12] IEEE Standard 519-1992, Recommended practices and requirements for harmonic control in electrical power systems, The Institute of Electrical and Electronics Engineers, 1993. (Standards and Reports)

INTERNATIONAL JOURNAL OF ENGINEERING TECHNOLOGIES (IJET)
COPYRIGHT AND CONSENT FORM

This form is used for article accepted to be published by the IJET. Please read the form carefully and keep a copy for your files.

TITLE OF ARTICLE (hereinafter, "The Article"):

……..…….....……

……..…….....……

……...……...……

LIST OF AUTHORS:

……..……...…..……

……..…….....……

……...……...……

CORRESPONDING AUTHOR'S ("The Author") NAME, ADDRESS, INSTITUTE AND EMAIL:

……...……

……..…….....……

……...……...……..…

COPYRIGHT TRANSFER

The undersigned hereby transfers the copyright of the submitted article to International Journal of Engineering Technologies (the "IJET"). The Author declares that the contribution and work is original, and he/she is authorized by all authors and/or grant-funding agency to sign the copyright form. Author hereby assigns all including but not limited to the rights to publish, distribute, reprints, translates, electronic and published derivates in various arrangements or any other versions in full or abridged forms to IJET. IJET holds the copyright of Article in its own name.

Author(s) retain all rights to use author copy in his/her educational activities, own websites, institutional and/or funder's web sites by providing full citation to final version published in IJET. The full citation is provided including Authors list, title of the article, volume and issue number, and page number or using a link to the article in IJET web site. Author(s) have the right to transmit, print and share the first submitted copies with colleagues. Author(s) can use the final published article for his/her own professional positions, career or qualifications by citing to the IJET publication.

Once the copyright form is signed, any changes about the author names or order of the authors listed above are not accepted by IJET.

Authorized/Corresponding Author **Date/ Signature**